

CHAPTER 4

RESULTS

The present study dealt with the identification of metabolites from pyrene and fluoranthene degradation via co-metabolism with phenanthrene by *Sphingomonas* sp. P2. The organism was found to be capable of utilizing phenanthrene as sole source of carbon and energy and possessed possibility to co-metabolize pyrene and fluoranthene using phenanthrene as growth substrate (Appendix F). Due to the fact that the organism could produce activities toward various substrates, thus, genes involved in this degradation were then studied.

To identify metabolites from the degradation of such compounds, large-scale cultivation using two 30-litre fermenters were carried out. Solvent extraction, silica gel open column, thin-layer and high performance liquid chromatography were used to isolate and purify the metabolites. Structure elucidation based on data obtained from gas chromatography-mass spectral, proton and carbon nuclear magnetic resonance spectral analyses were performed.

4.1 Identification of metabolites from degradation of pyrene via co-metabolism with phenanthrene by *Sphingomonas* sp. P2

4.1.1 Partial purification of metabolites by silica gel open column chromatography

After cultivation of *Sphingomonas* sp. P2 in CFMM/phe/pyr for 4 days; bacterial cells separation was performed. Five liters of supernatant was extracted with ethyl acetate according to the procedure shown in Figure 3.2. The acidic extract obtained (875 mg) was partially purified by silica gel open column chromatography. Twelve fractions collected (Table 4.1) were dehydrated over anhydrous Na_2SO_4 and evaporated to 10 ml then characterized via TLC to identify fractions containing metabolites (results are depicted in Figure 4.1).

Table 4.1 Dry weight of each fraction obtained from silica gel open column chromatography of the acidic extract

Fraction	Eluent (%by volume)		Dry weight (mg)
	<i>n</i> -Hexane	Ethyl acetate	
1	100	0	0.02
2	90	10	5.22
3	80	20	7.04
4	70	30	20.10
5	60	40	82.95
6	50	50	47.74
7	40	60	172.31
8	30	70	135.05
9	20	80	41.64
10	10	90	18.44
11	0	100	7.19
12	100% Methanol		45.18

สถาบันวิทยบริการ
จุฬาลงกรณ์มหาวิทยาลัย

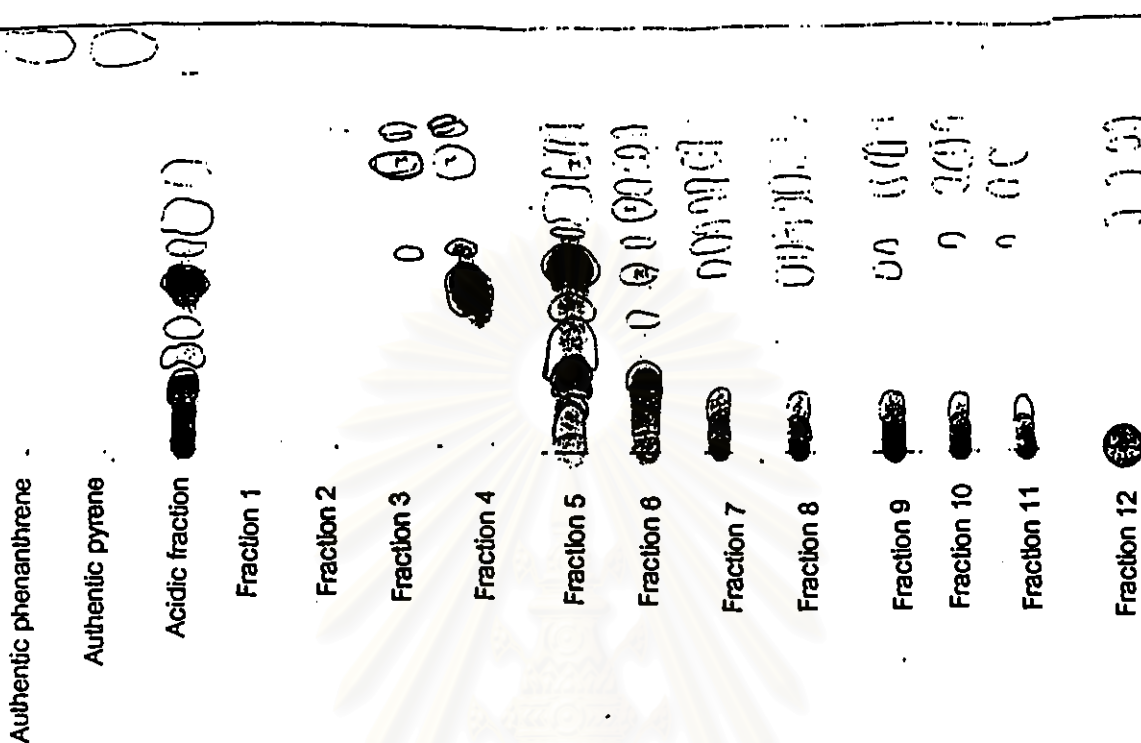


Figure 4.1 TLC chromatogram of each fraction after partial purification by silica gel open column chromatography. TLC-developing solvent system was toluene, dioxane and acetic acid (90:25:4,v/v/v).

TLC analysis revealed the presence of metabolites were found in all fractions. The major metabolites were found in fraction 4 (70% hexane) and fraction 5 (60% hexane), respectively. However, based on the TLC chromatogram, the fractions were combined as follows: fractions 3 with 4 as F1 and fractions 7 with 8 as F4, while fractions 5, 6 and 9 were collected separately and designated as F2, F3 and F5, respectively.

4.1.2 Purification of the metabolites by HPLC

The fractions collected were evaporated to dryness and redissolved in methanol to the concentration of 1 mg/10 μ l.

These fractions were subjected to reversed phase HPLC using with linear gradient solvent system for the elution. The HPLC elution profiles are shown in Figure

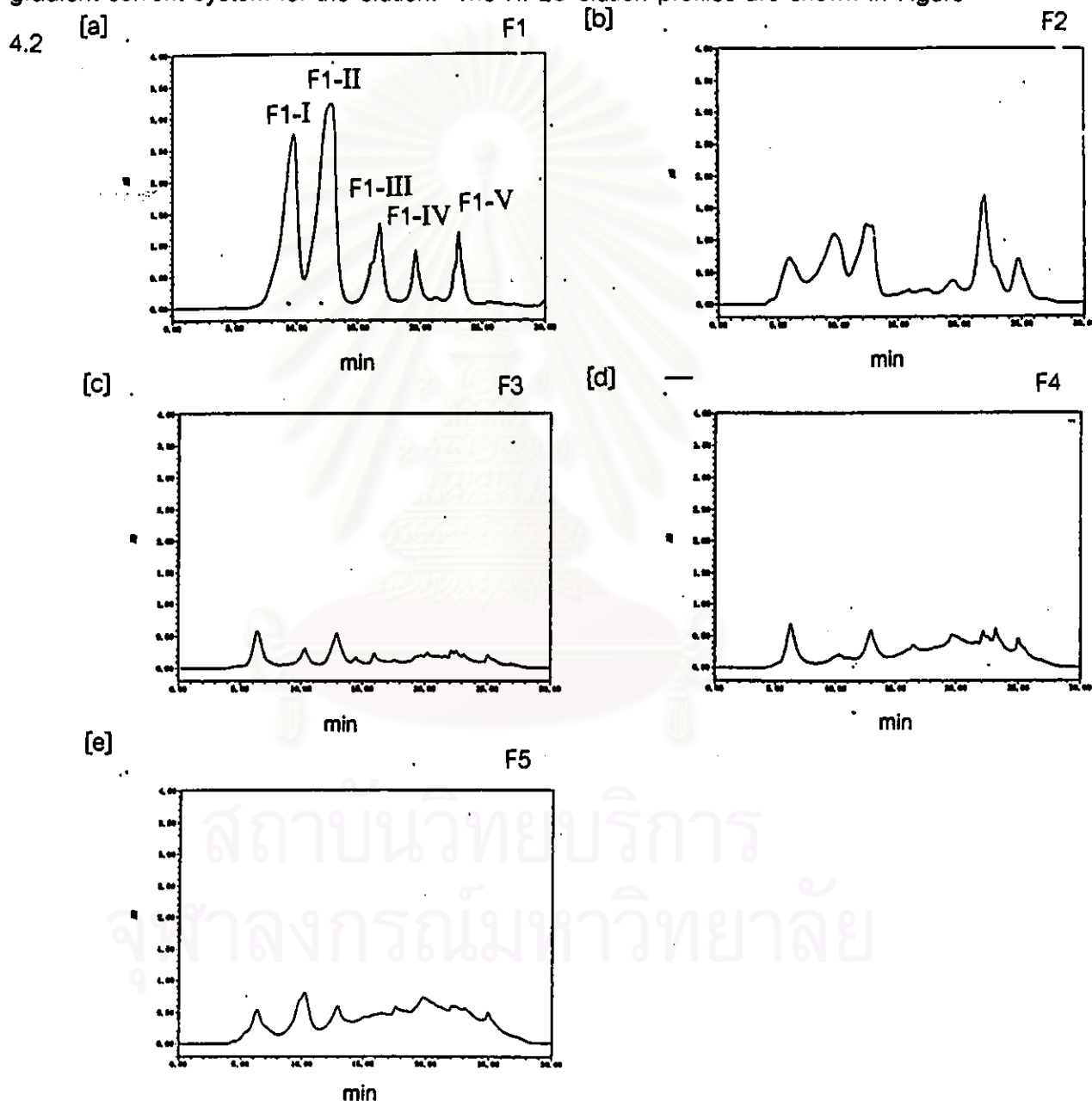


Figure 4.2 HPLC chromatograms of fractions F1 to F5 applied onto an ODS-4253-D column eluted with a methanol-water linear gradient solvent system (50 to 100 % [v/v] methanol containing 1% acetic acid)

The HPLC chromatograms indicated that fractions F1 and F2 contained substantial amount of metabolites with well separated. Individual peak of F1 and F2 fraction separated by HPLC were collected and further analyzed by TLC as shown in Figures 4.3 and 4.4.

[a]

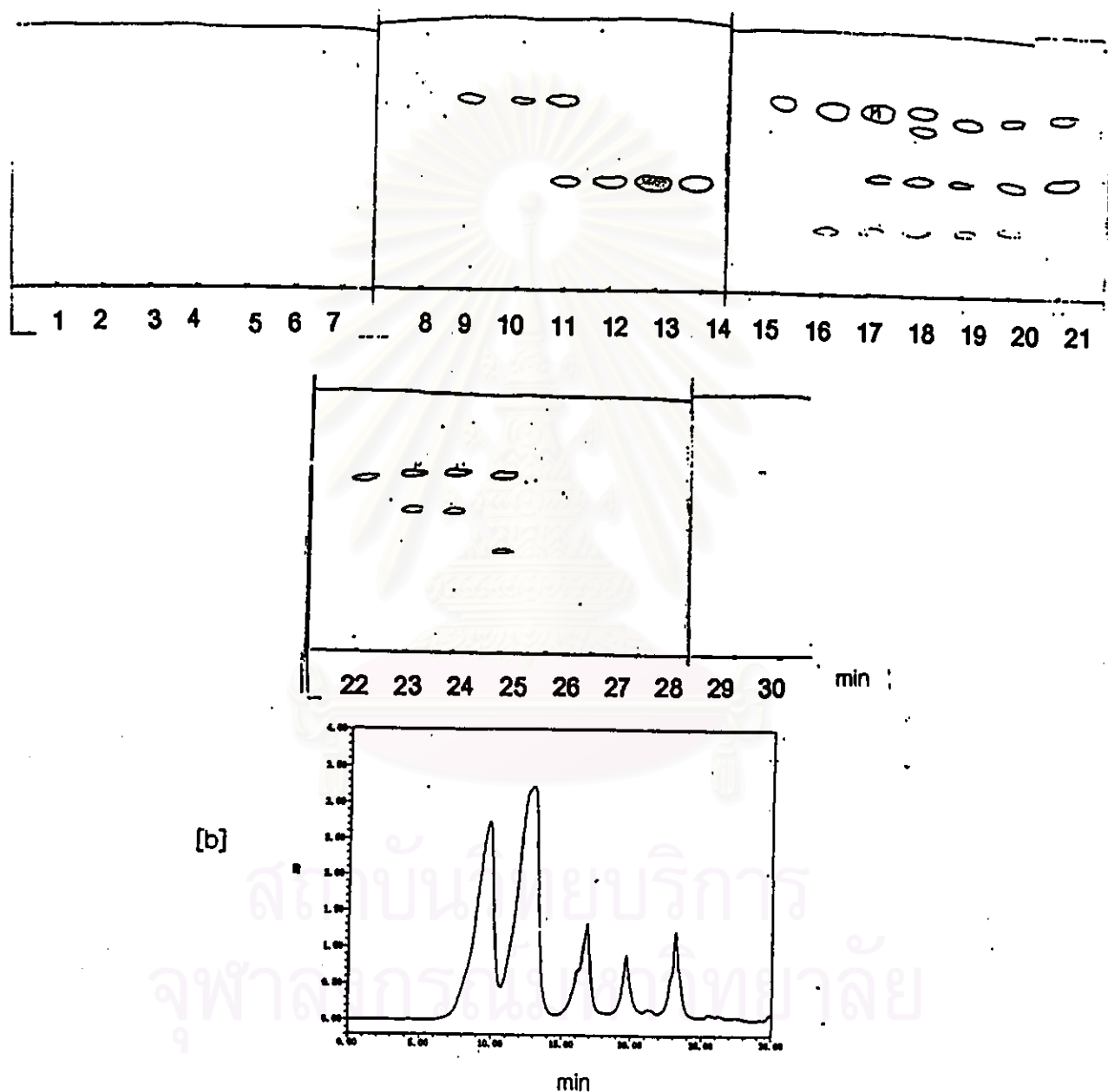


Figure 4.3 [a] TLC chromatograms of F1-eluate fractions purified by HPLC as shown in Figure 4.2 collected every 1 min for 30 min; [b] HPLC elution profile of the analyzed fractions

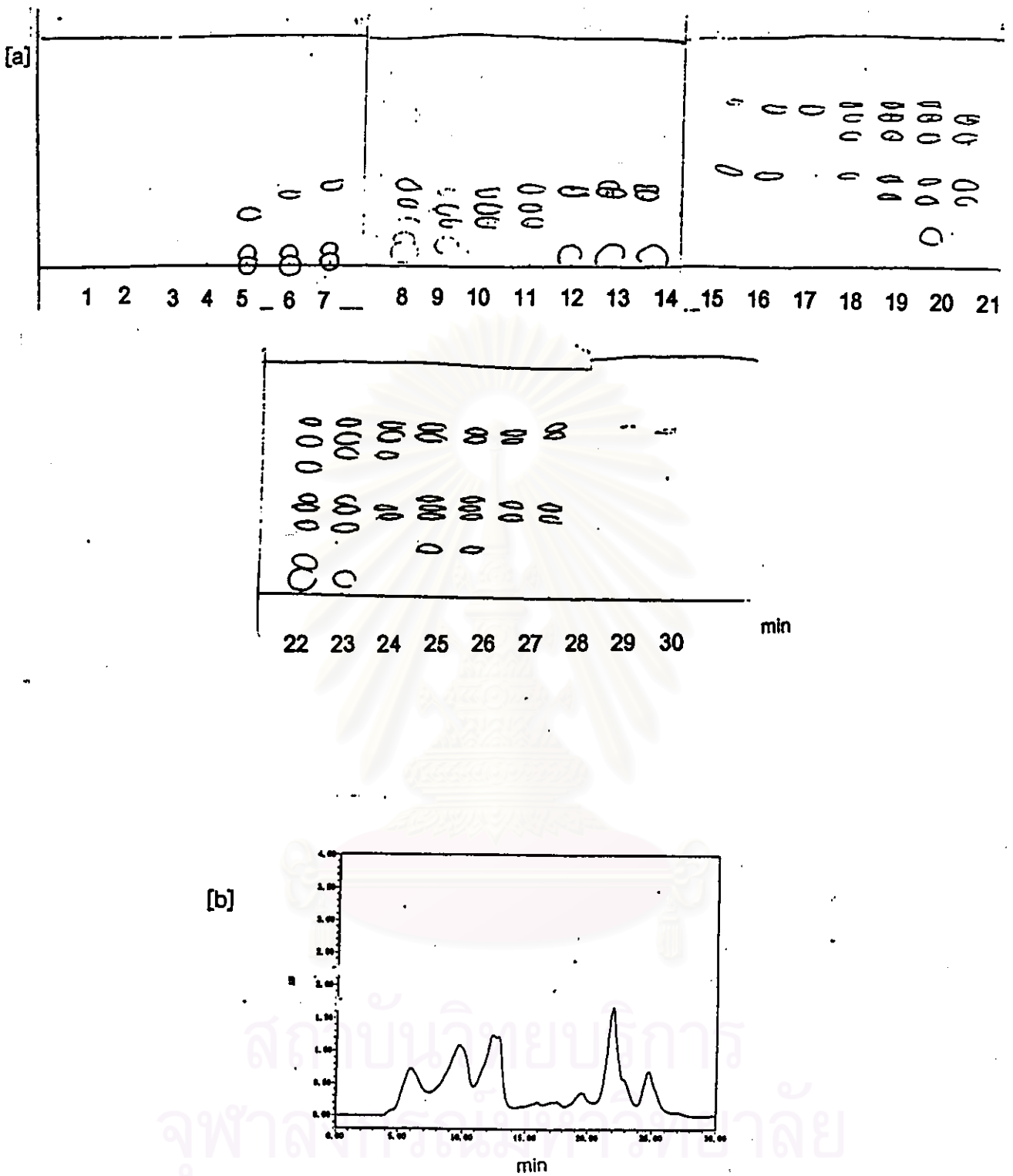


Figure 4.4 [a] TLC chromatograms of F2-eluate fractions purified by HPLC as shown in Figure 4.2 collected every 1 min for 30 min; [b] HPLC elution profile of the analyzed fractions

From HPLC and TLC analyses, fraction F1 was chosen for further characterization due to its high purity.

Five peaks were obtained when fraction F1 was subjected to HPLC which were designated as F1-I, F1-II, F1-III, F1-IV and F1-V with the corresponding retention times of 10, 13, 17, 19.8 and 23.2 min, respectively (Figure 4.2a). From TLC analyses in Figure 4.3, F1-II, F1-III, F1-IV and F1-V were still not homogeneous, thus, were then subjected to further purification via reverse phase and normal phase HPLC by the use of isocratic solvent system.

Six separated fractions designated as F1-IIa and F1-IIb from fraction F1-II, F1-IIIa and F1-IIIb from fraction F1-III and F1-IVa and F1-IVb from fraction F1-IV, were obtained as depicted in Figures 4.5, 4.6 and 4.7, respectively. Conditions of mobile phase and the retention times of the eluted compounds are demonstrated in Table 4.2. Repeated injection into HPLC with subsequent collection of metabolite peaks was conducted to accumulate the purified fractions.

For F1-V, it was found that this fraction was unstable in the storage condition, therefore further purification and structural analyses could not be done.

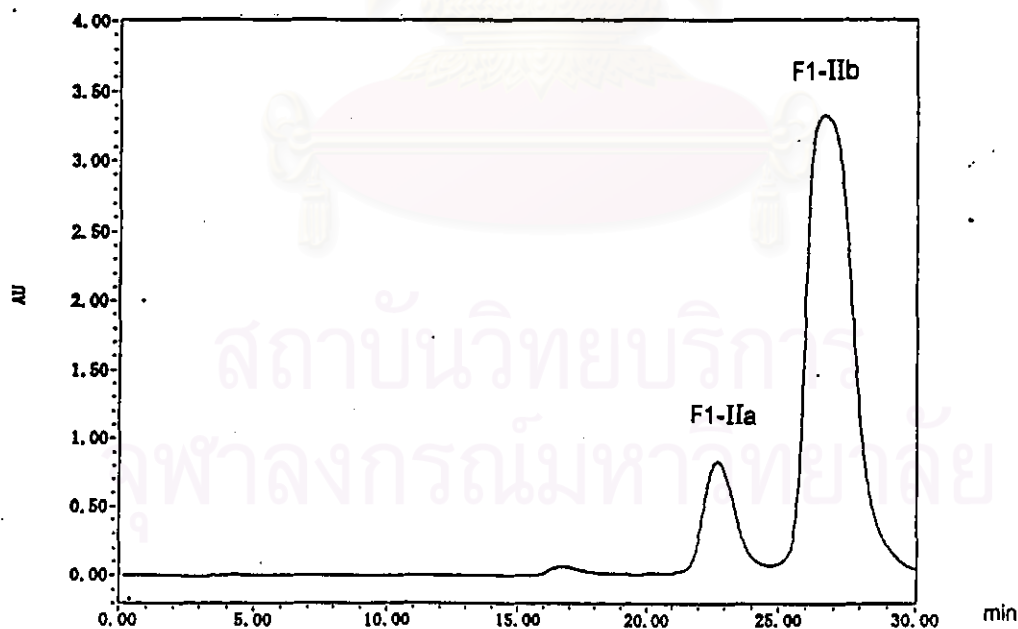


Figure 4.5 HPLC elution profile of fraction F1-II showing the separation of fractions F1-IIa and F1-IIb on reversed phase HPLC system with isocratic methanol-water-acetic acid [45:55:1, v/v/v] solvent system

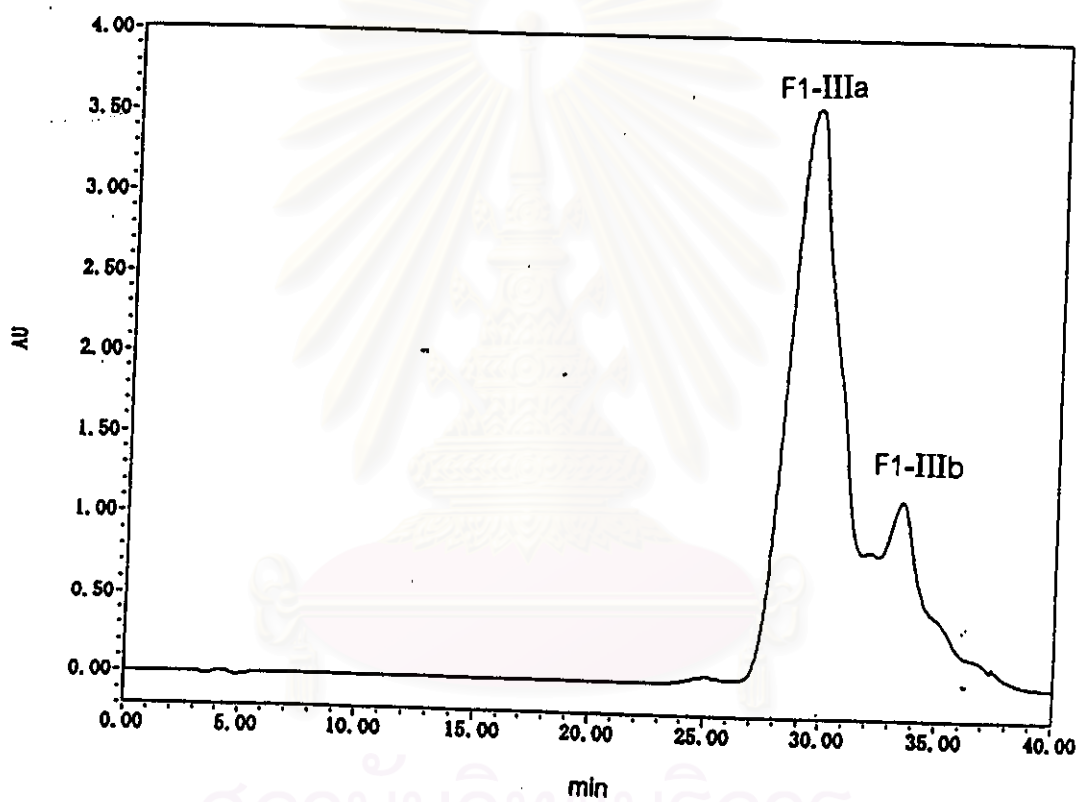
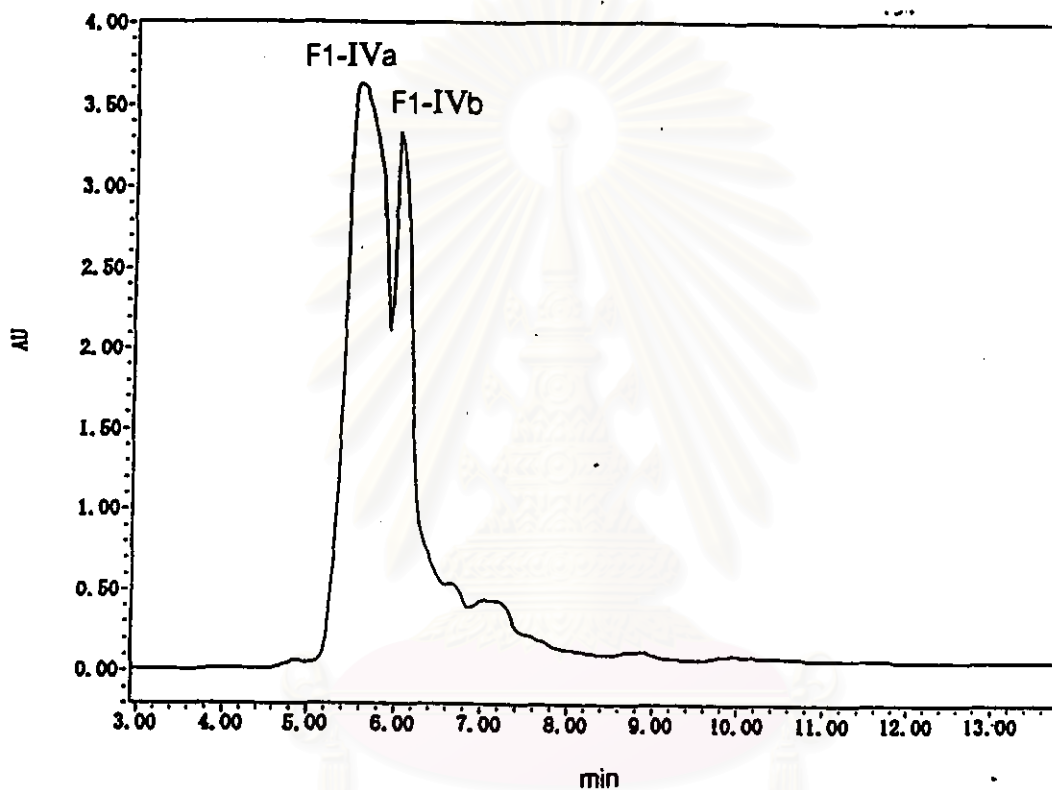


Figure 4.6 HPLC elution profile of fraction F1-III showing the separation of fractions F1-IIIa and F1-IIIb on reversed phase HPLC system with isocratic methanol-water-acetic acid [50:50:1, v/v/v] solvent system



สถาบันวิทยบริการ
จุฬาลงกรณ์มหาวิทยาลัย

Figure 4.7 HPLC elution profile of fraction F1-IV showing the separation of fractions F1-IVa and F1-IVb on normal phase HPLC system with isocratic *n*-hexane-isopropanol-acetic acid [95:5:1, v/v/v] solvent system

Table 4.2 HPLC separations of fractions F1-I, F1-IIa, F1-IIb, F1-IIIa, F1-IIIb, F1-IVa and F1-IVb with their mobile phase systems used in each purification process as well as their retention times of elution and dry weight

Fractions	Mobile phase	Retention time (min)	Dry weight (mg)
F1-I	Methanol-water linear gradient solvent system (50 to 100% [v/v] methanol with 1% acetic acid in 30 min) ^a	10.0	2.34
F1-IIa	Isocratic methanol-water-acetic acid [45:55:1, v/v/v] ^a	22.8	0.98
F1-IIb	Isocratic methanol-water-acetic acid [45:55:1, v/v/v] ^a	26.9	3.92
F1-IIIa	Isocratic methanol-water-acetic acid [50:50:1, v/v/v] ^a	29.5	0.045
F1-IIIb	Isocratic methanol-water-acetic acid [50:50:1, v/v/v] ^a	33.5	0.024
F1-IVa	Isocratic <i>n</i> -hexane-isopropanol-acetic acid [95:5:1, v/v/v] ^b	5.6	0.015
F1-IVb	Isocratic <i>n</i> -hexane-isopropanol-acetic acid [95:5:1, v/v/v] ^b	6.1	-

^aReversed phase HPLC system

^bNormal phase HPLC system

4.1.3 Structure elucidation of metabolites via GC-MS and NMR

Fractions F1-I, F1-IIb, F1-IIIa, F1-IIIb and F1-IVa were characterized for their structures by GC-MS and NMR analyses.

Metabolite F1-I

Metabolite F1-I had the molecular ion (M^+) at m/z 146 and fragmentation ions at m/z 118 ($M^+ - 28$, CO loss) and m/z 90 ($M^+ - 56$, further CO loss) (Figure 4.8 and Table 4.7). This MS analysis of metabolite F1-I is consistent with a molecular formula of $C_9H_6O_2$.

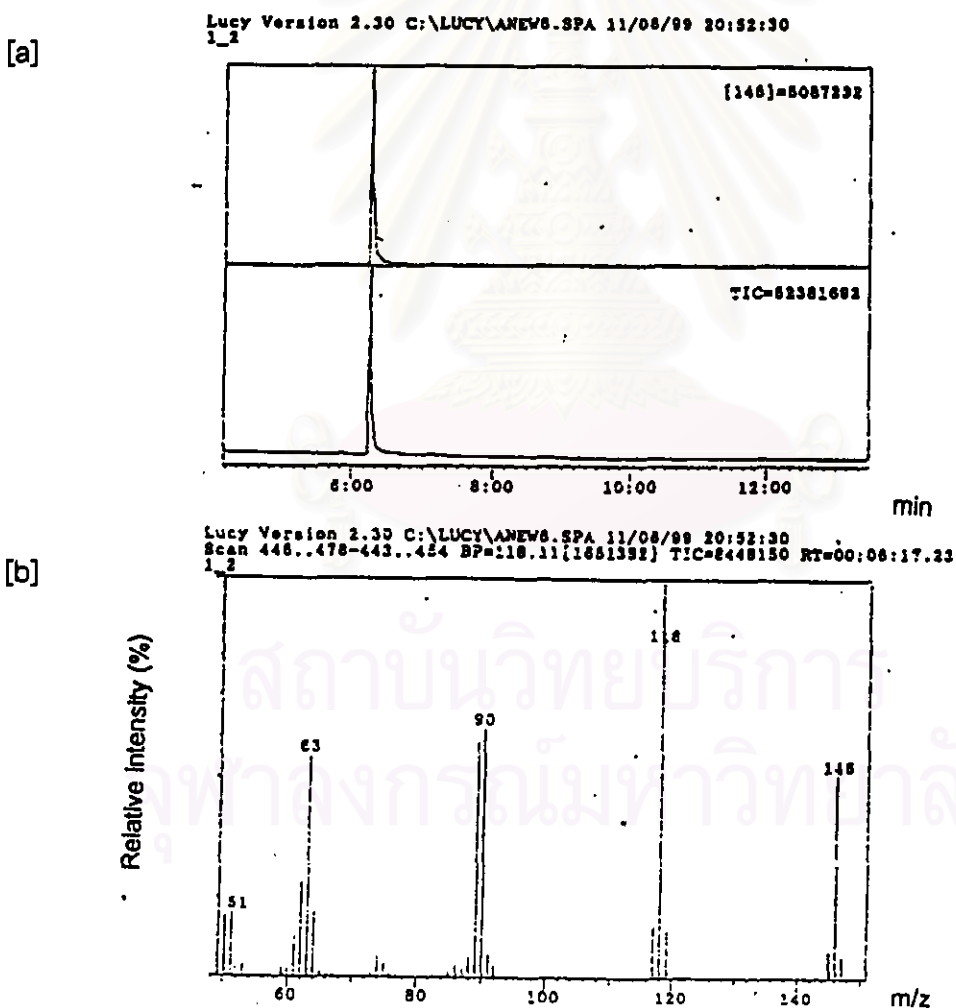


Figure 4.8 [a] Total ion chromatogram and [b] mass spectrum of metabolite F1-I formed from phenanthrene degradation by *Sphingomonas* sp. P2 grown in the presence of pyrene

^1H NMR spectrum of metabolite F1-I was identical to that of authentic coumarin as described in Table. 4.3 and Figure 4.9.

Table 4.3 ^1H NMR spectral data for metabolite F1-I and authentic coumarin

Protons	δ_{H} (ppm)	
	Metabolite F1-I CDCl ₃ , 500 MHz	Coumarin ^a CDCl ₃ , 399.65 MHz
H-3	6.45 (d)	6.42 (d)
H-4	7.77 (d)	7.72 (d)
H-5	7.52 (d)	7.50 (d)
H-6	7.30 (t)	7.28 (t)
H-7	7.56 (t)	7.53 (t)
H-8	7.36 (d)	7.32 (d)

^aFrom database 'Aldrich Library of ^1H NMR spectra'

สถาบันวิทยบริการ
จุฬาลงกรณ์มหาวิทยาลัย

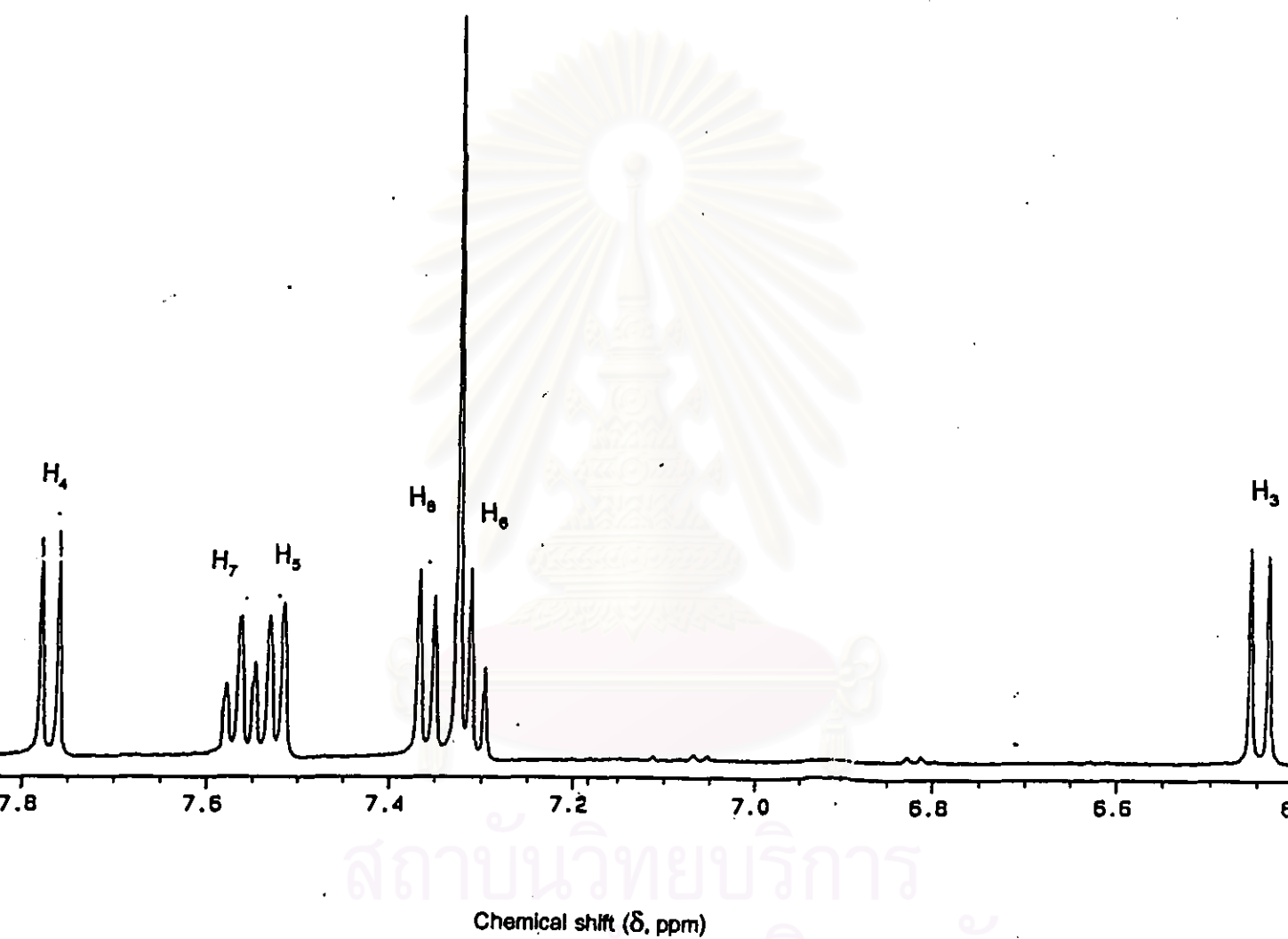


Figure 4.9 $^1\text{H-NMR}$ spectrum of metabolite F1-I formed from phenanthrene degradation by *Sphingomonas* sp. P2 grown in the presence of pyrene

From GC-MS and $^1\text{H-NMR}$ spectra, F1-I shown similarity to authentic coumarin, then it was identified as coumarin (Figure 4.10).

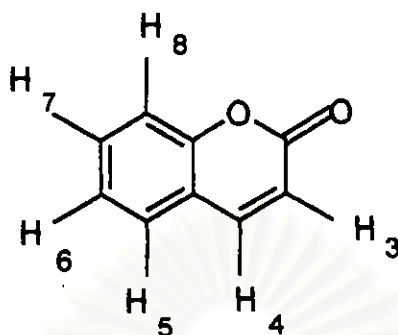


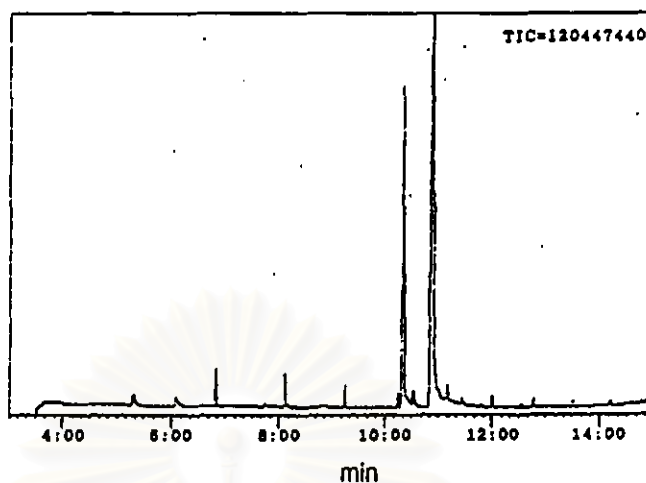
Figure 4.10 Structure of metabolite F1-I which has the identical properties to those of the coumarin

Metabolite F1-IIb

From GC-MS analyses of methylated derivative of metabolite F1-IIb (a major metabolite), two components with the retention times (R_t) of 10.2 and 10.5 min were detected as shown in Figure 4.11a. The mass spectrum of the latter compound (a major compound) exhibited molecular ion (M^+) at m/z 218 (monomethyl derivative of F1-IIb) and fragmentation ions at m/z 186 ($M^+ - \text{CH}_3\text{OH}$), m/z 168, 158, 130, 102 and 77 (Figure 4.11b). While the mass spectrum of another compound showed molecular ion (M^+) at m/z 232 (dimethyl derivative of F1-IIb) and fragmentation ions at m/z 200 ($M^+ - \text{CH}_3\text{OH}$), m/z 185 ($M^+ - \text{CH}_3\text{OH} - \text{CH}_3$), m/z 172 ($M^+ - \text{CH}_3\text{OH} - \text{CO}$) and m/z 157 ($M^+ - \text{CH}_3\text{OH} - \text{CO} - \text{CO}$) (Figure 4.11c). The results indicated the molecular formula of $\text{C}_{12}\text{H}_{10}\text{O}_4$ and $\text{C}_{13}\text{H}_{12}\text{O}_4$, respectively. Table 4.7 summarizes data obtained from GC-MS analysis of this compound.

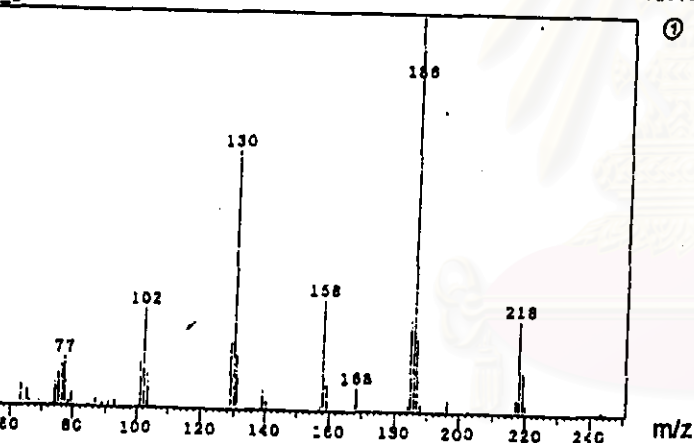
[a]

Lucy Version 2.30 C:\LUCY\ANWS.SPA 11/06/99 21:39:26
2.2_2



[b]

Lucy Version 2.30 C:\LUCY\ANWS.SPA 11/06/99 21:39:26
Scan 1110..1145-1112..1128 BP=186.17(162599) TIC=839535 RT=00:10:50.81



[c]

Lucy Version 2.30 C:\LUCY\ANWS.SPA 11/06/99 21:39:26
Scan 1012..1074-985..1012 BP=200.19(578920) TIC=4786047 RT=00:10:50.81

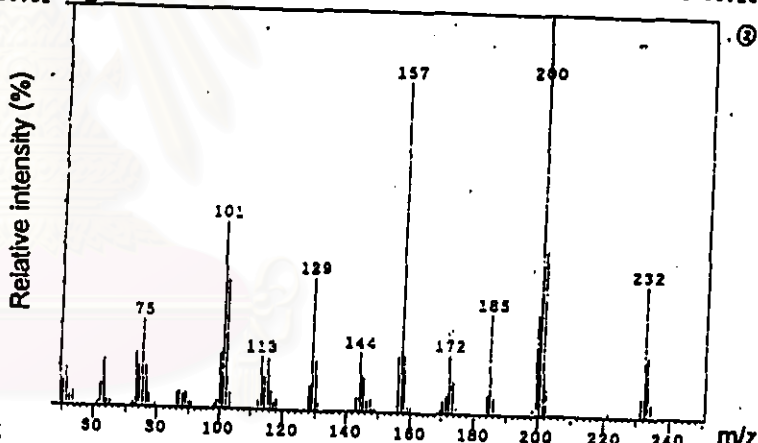


Figure 4.11 [a] Total ion chromatogram, [b] mass spectrum of monomethyl derivative of metabolite F1-IIb [c] mass spectrum of dimethyl derivative of metabolite F1-IIb formed from phenanthrene degradation by *Sphingomonas* sp. P2 grown in the presence of pyrene

The $^1\text{H-NMR}$ spectrum (Figures 4.12) of metabolite F1-IIb showed signal at δ 7.53-7.58 ppm and 7.11 ppm which were protons of aromatic ring ($=\text{CH-}$). The $^{13}\text{C-NMR}$ spectrum (Figures 4.13) of this compound showed ten signals of aromatic carbons at 105.2, 107.2, 117.9, 120.7, 122.2, 125.8, 129.0, 131.2, 154.6 and 159.1 ppm as well as one signal of carbon in carboxylic acid at 174.2 ppm.

Furthermore, information from two- dimensional NMR techniques; heteronuclear multiple quantum correlation (HMQC), heteronuclear multiple bond correlation (two- and three-bond) (HMBC) were also used to elucidate the structure of metabolite F1-IIb.

From HMQC spectra (Figure 4.14), five protons coupled with carbons of aromatic rings were elucidated (Table 4.4).

Table 4.4 The HMQC spectral data of metabolite F1-IIb

Position	HMQC	
	δ_{H}	δ_{C}
4	7.11 (2H, dd)	120.7
8		117.9
3	7.53-7.58 (3H, m)	122.2
6		105.2
7		129.0

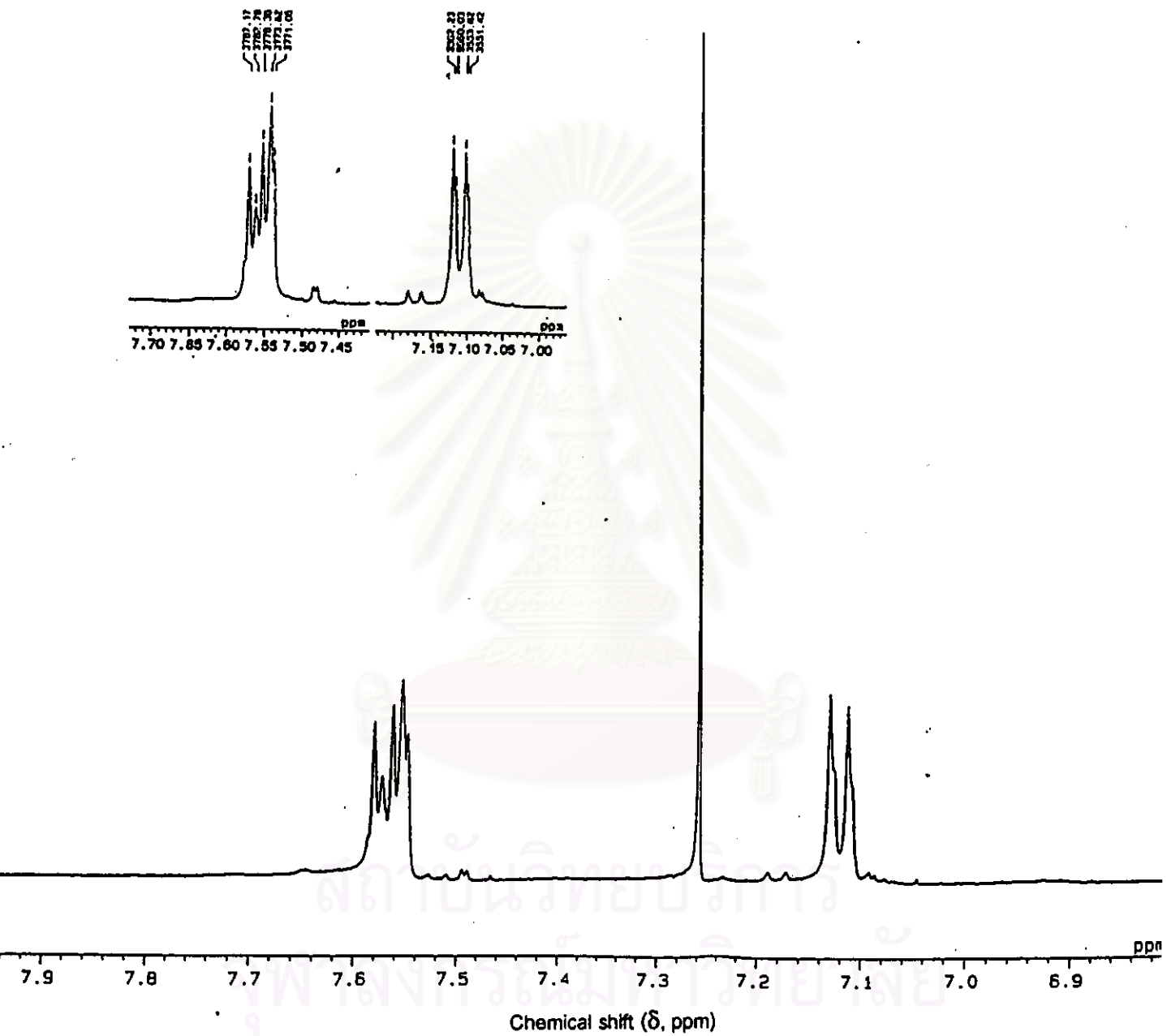


Figure 4.12 $^1\text{H-NMR}$ spectrum of metabolite F1-IIb formed from phenanthrene degradation by *Sphingomonas* sp. P2 grown in the presence of pyrene

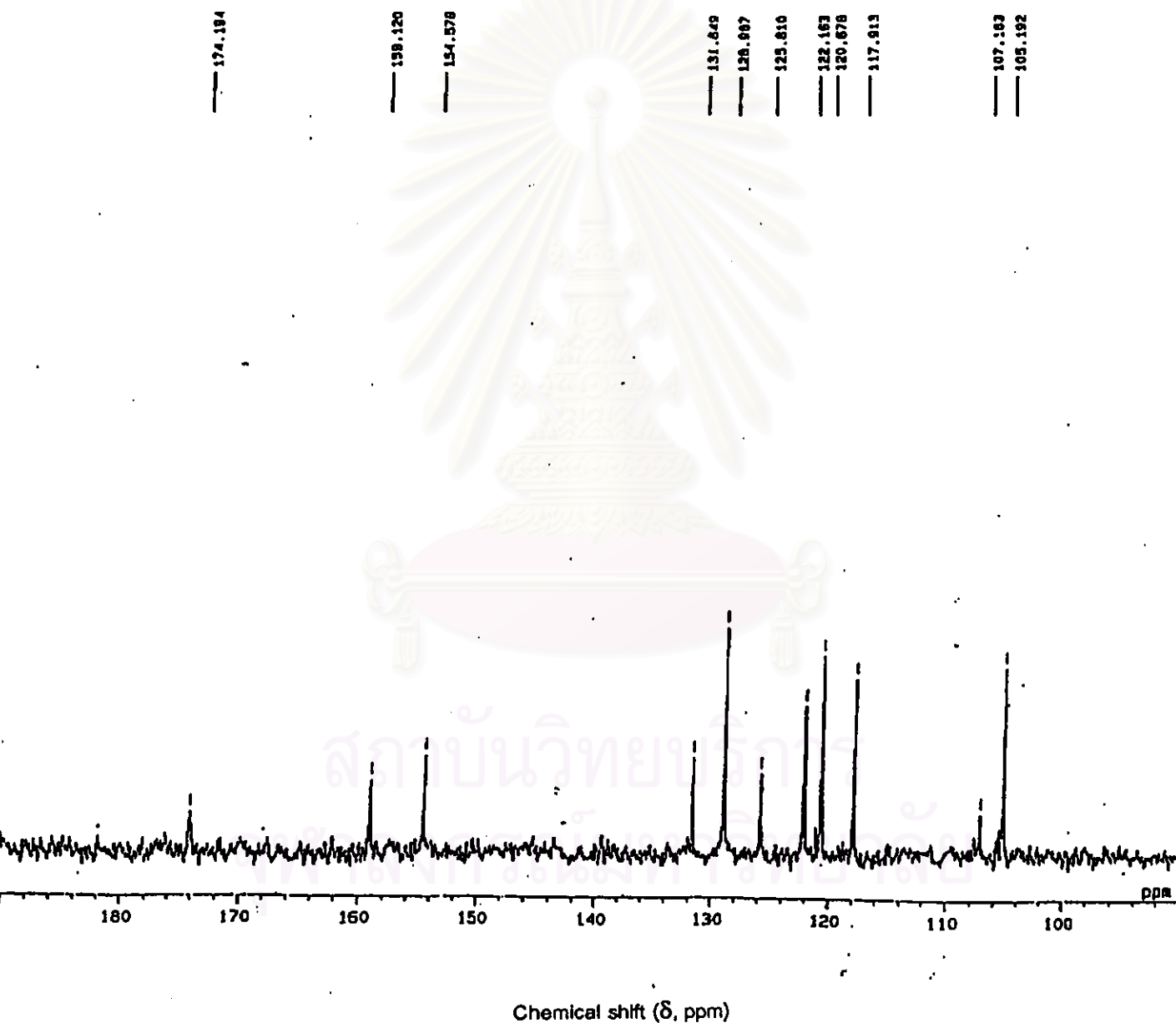


Figure 4.13 ^{13}C -NMR spectrum of metabolite F1-IIb formed from phenanthrene degradation by *Sphingomonas* sp. P2 grown in the presence of pyrene

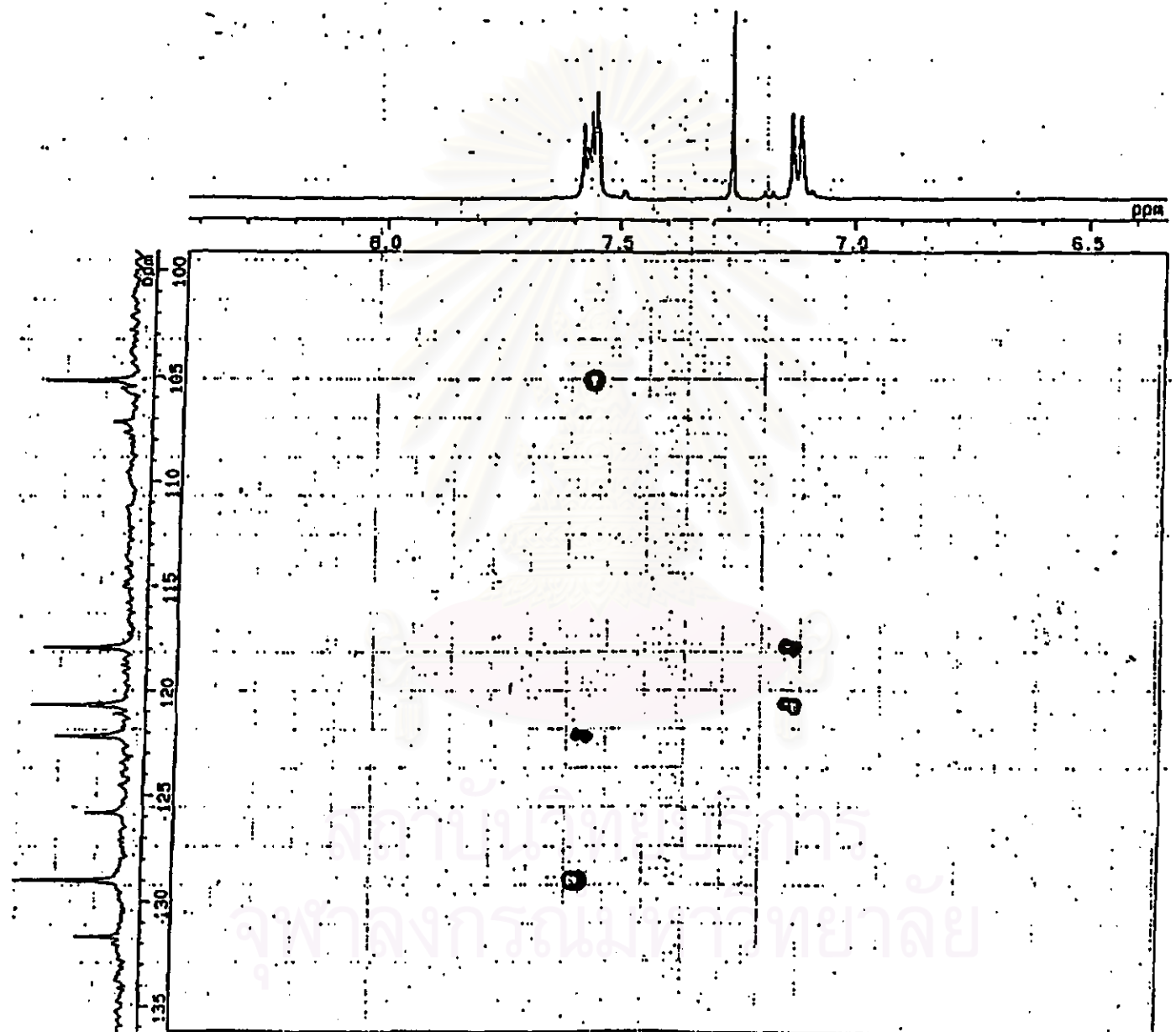


Figure 4.14 HMQC data of metabolite F1-IIb formed from phenanthrene degradation by *Sphingomonas* sp. P2 grown in the presence of pyrene

Comparison of structure of metabolite F1-IIb and that of resemble compound (1-hydroxy-2-naphthoic acid) was done in order to assign structure of this metabolite (Figure 4.15).

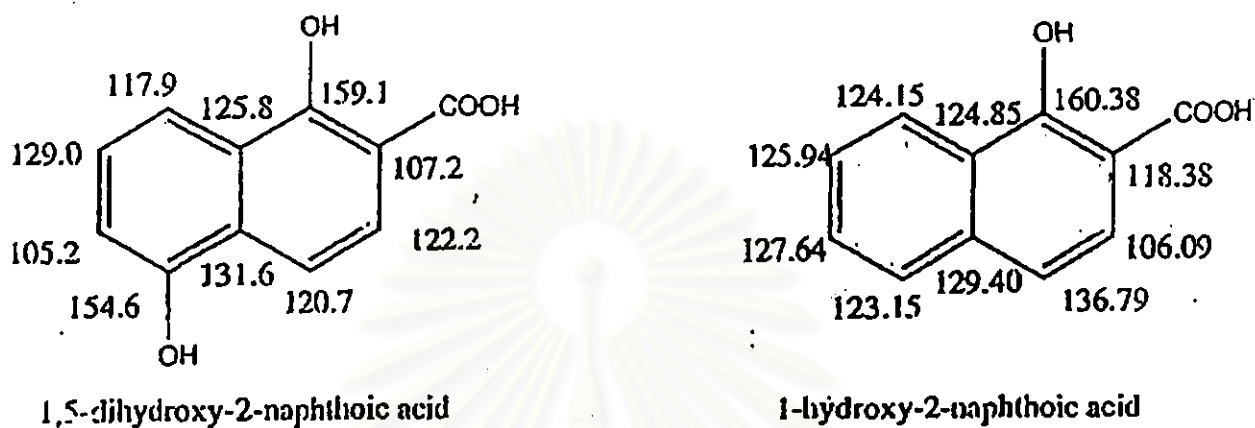


Figure 4.15 Assignment for structure of metabolite F1-IIb by comparison with that of 1-hydroxy-2-naphthoic acid

The long-range ^1H - ^{13}C correlations as shown in Figure 4.16 obtained by HMBC experiment (Figures 4.17) confirmed that the structure of compound F1-IIb corresponded with those of 1,5-dihydroxy-2-naphthoic acid.

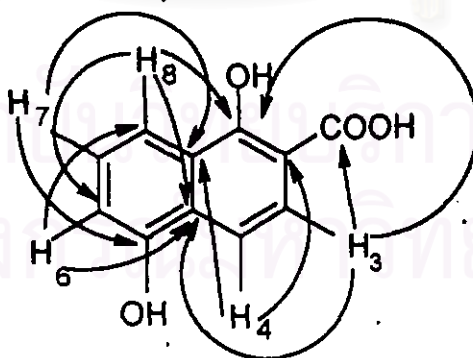


Figure 4.16 The HMBC correlations of metabolite F1-IIb

Consequently, structure of metabolite F1-IIb was determined to be 1,5-dihydroxy-2-naphthoic acid.

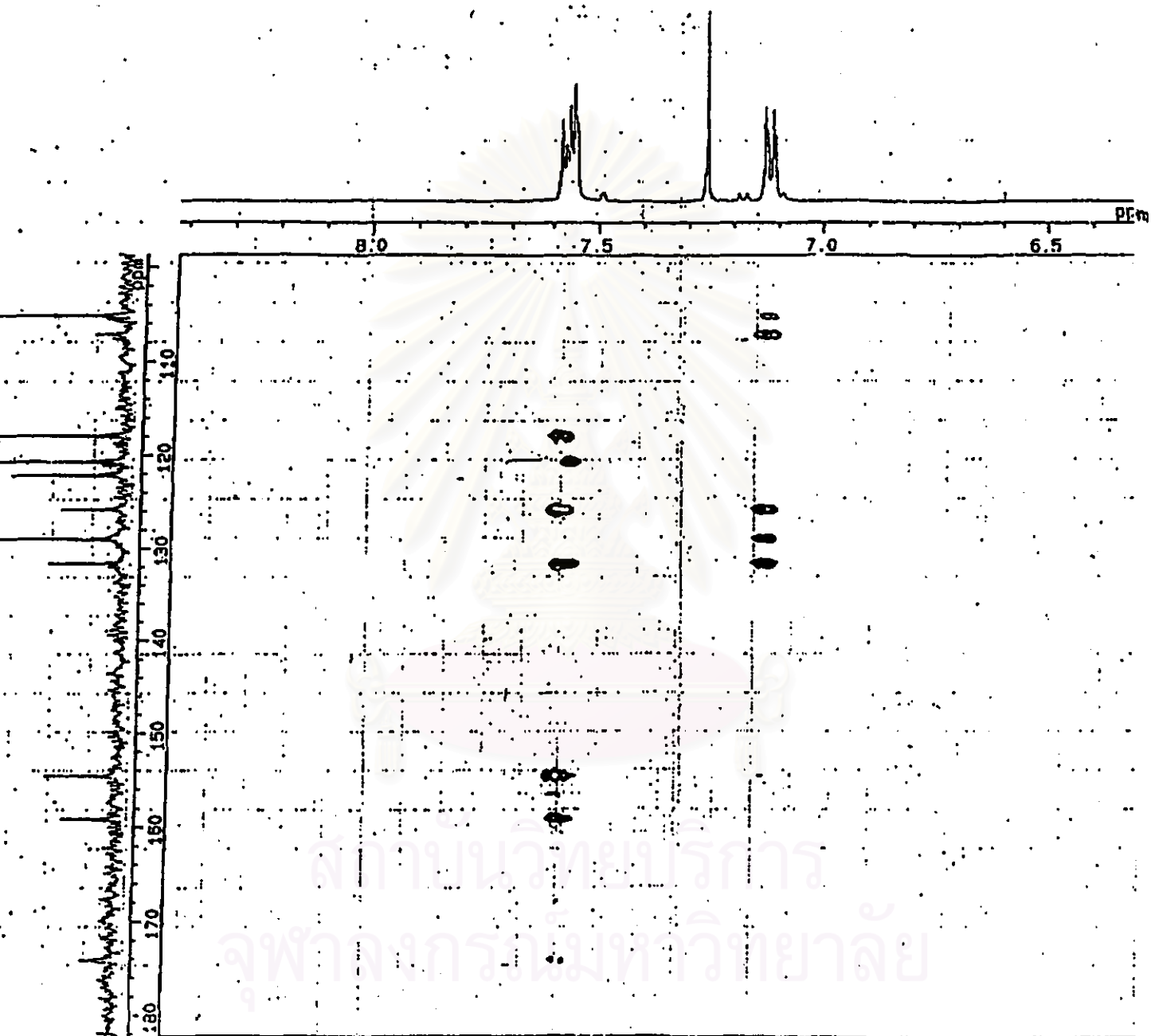
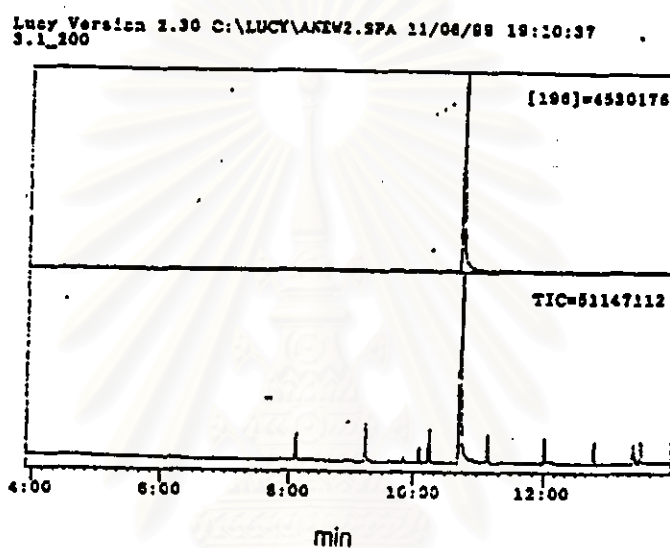


Figure 4.17 HMBC data of metabolite F1-IIb formed from phenanthrene degradation by *Sphingomonas* sp. P2 grown in the presence of pyrene

Metabolites F1-IIIa and F1-IIIb

GC-MS analysis of metabolites F1-IIIa and F1-IIIb (Figures 4.18 and 4.19) suggested that both metabolites had the molecular ion (M^+) at m/z 196 and fragment ions at m/z 168 (M^+-28) and m/z 139 (M^+-57), representing probable losses of CO and CO plus CHO, respectively. The GC-MS data of this compound are also summarized in Table 4.7

[a]



[b]

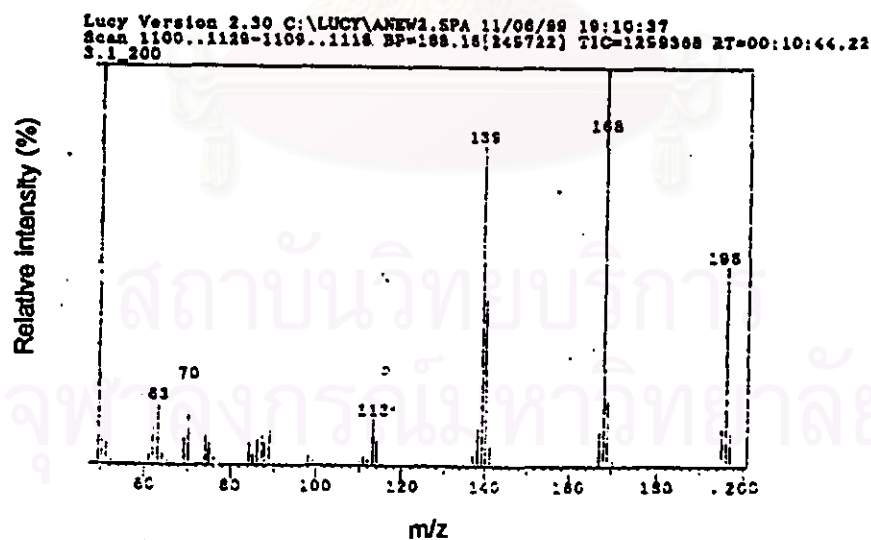
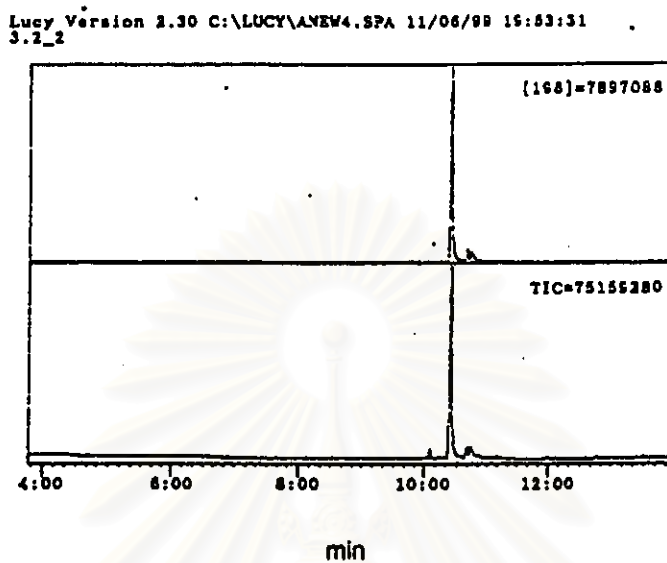


Figure 4.18 [a] Total ion chromatogram and [b] mass spectrum of metabolite F1-IIIa formed from phenanthrene degradation by *Sphingomonas* sp. P2 grown in the presence of pyrene

[a]



[b]

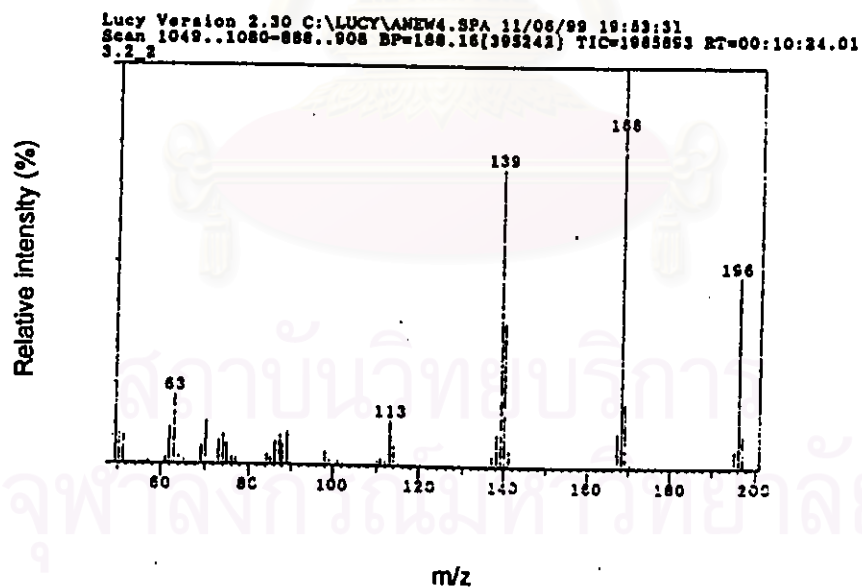


Figure 4.19 [a] Total ion chromatogram and [b] mass spectrum of metabolite F1-IIIb formed from phenanthrene degradation by *Sphingomonas* sp. P2 grown in the presence of pyrene

The $^1\text{H-NMR}$ spectrum of metabolites F1-IIIa and F1-IIIb showed signals between δ 6.55-8.54 ppm (Figure 4.20) and 6.49-8.50 ppm (Figure 4.21), respectively which corresponded to protons of aromatic rings ($=\text{CH-}$). Moreover, information from Two-dimensional NMR techniques; $^1\text{H-}^1\text{H}$ shift- correlated spectroscopy ($^1\text{H-}^1\text{H}$ COSY), nuclear overhauser enhancement spectroscopy (NOESY), HMQC and HMBC experiments were used to assist structure interpretation of metabolites F1-IIIa and F1-IIIb.

According to $^1\text{H-}^1\text{H}$ COSY spectral data (Figures 4.22 and 4.23), possible structures of both metabolites are presented in Figure 4.24.

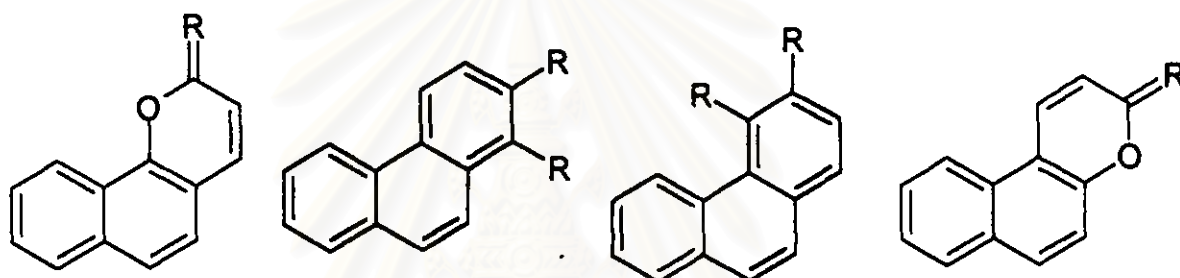


Figure 4.24 Possible structures of metabolites F1-IIIa and F1-IIIb (R = non H moiety)

The mass spectral fragmentation patterns suggested that metabolites F1-IIIa and F1-IIIb might be benzocoumarin-like compounds (Figure 4.25).

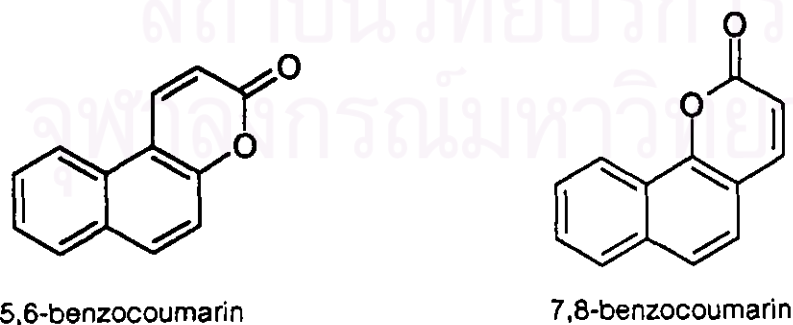


Figure 4.25 Benzocoumarin compounds

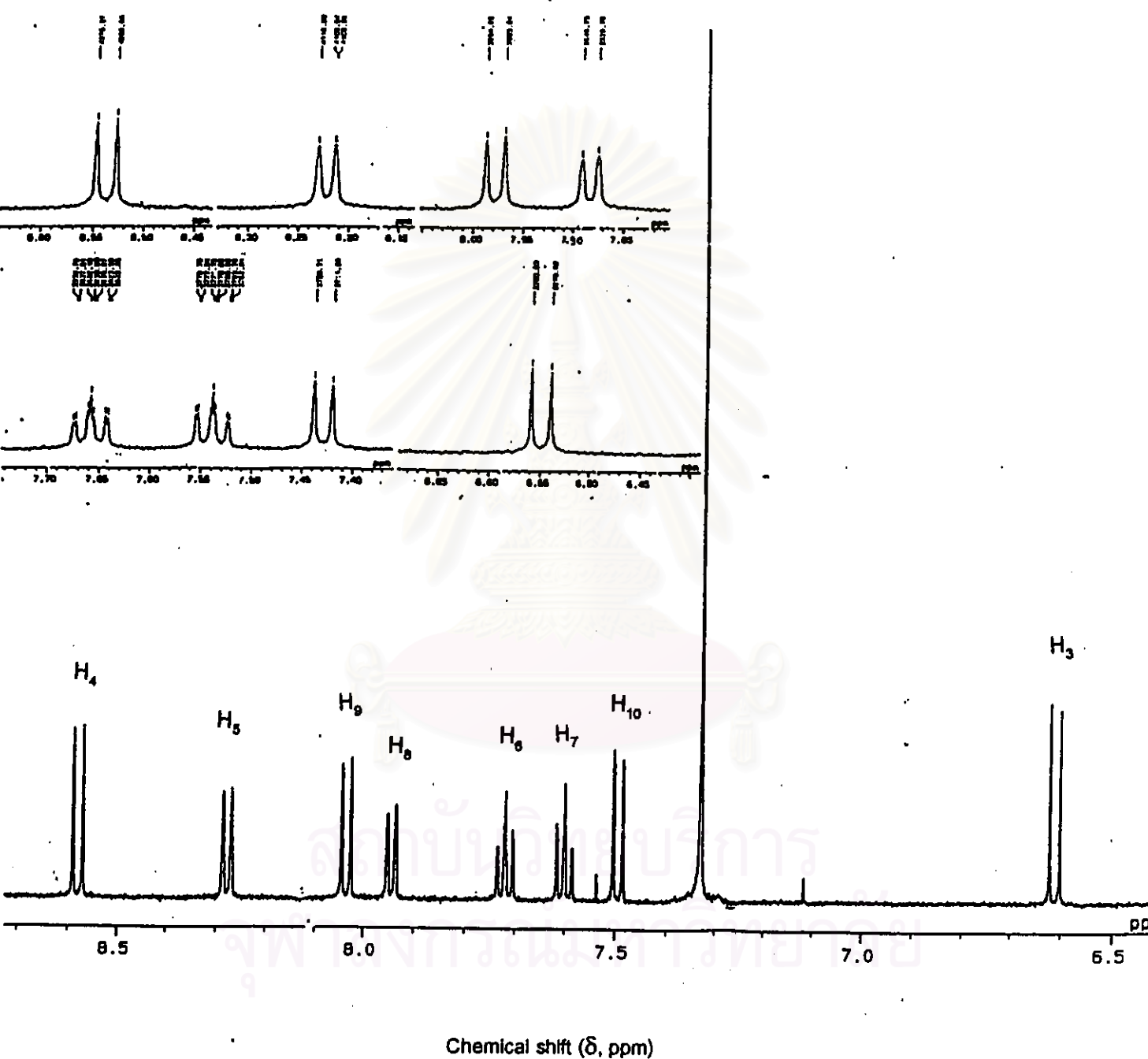


Figure 4.20 $^1\text{H-NMR}$ spectrum of metabolite F1-IIIa formed from phenanthrene degradation by *Sphingomonas* sp. P2 grown in the presence of pyrene

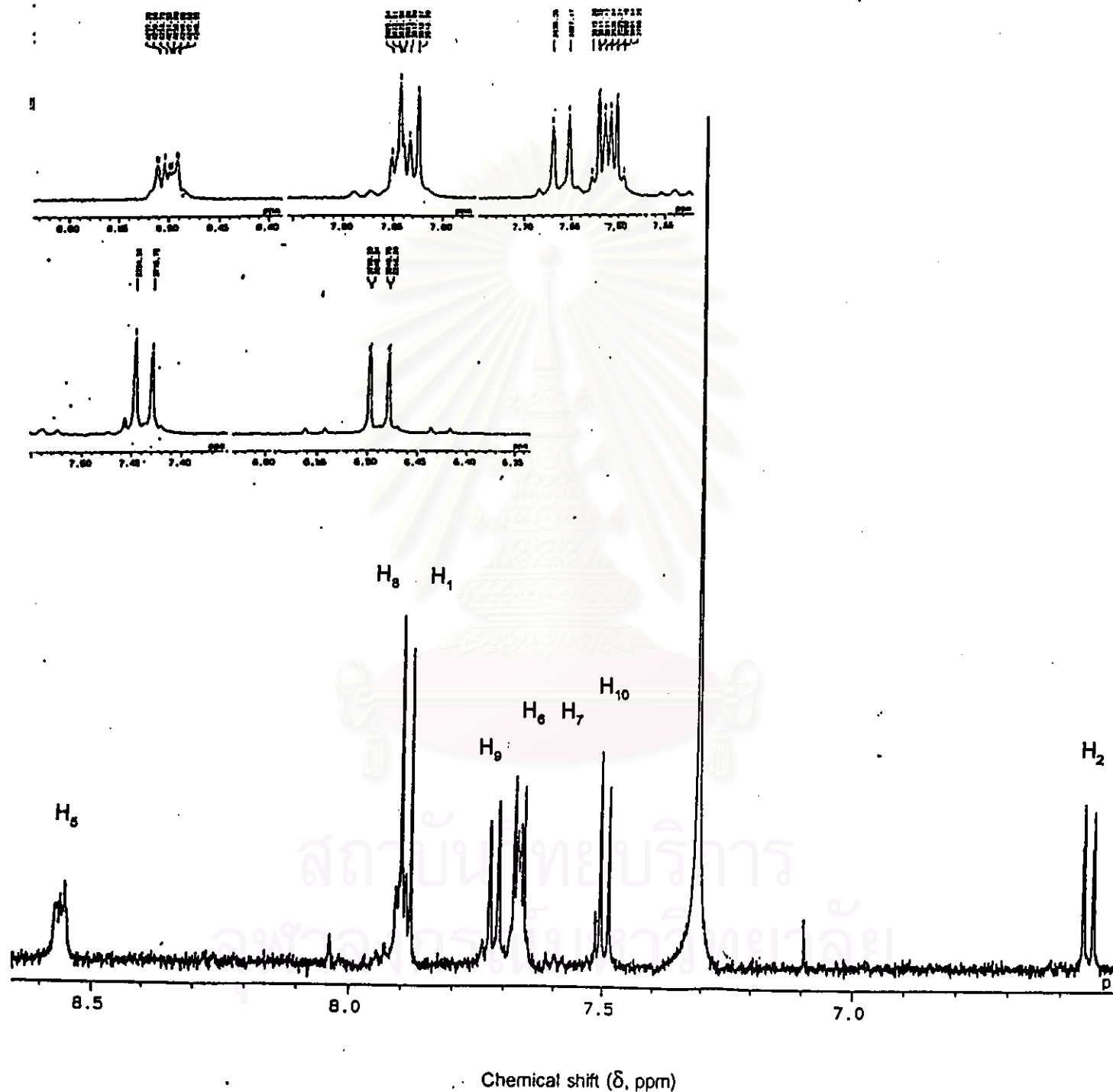


Figure 4.21 $^1\text{H-NMR}$ spectrum of metabolite F1-IIIb formed from phenanthrene degradation by *Sphingomonas* sp. P2 grown in the presence of pyrene

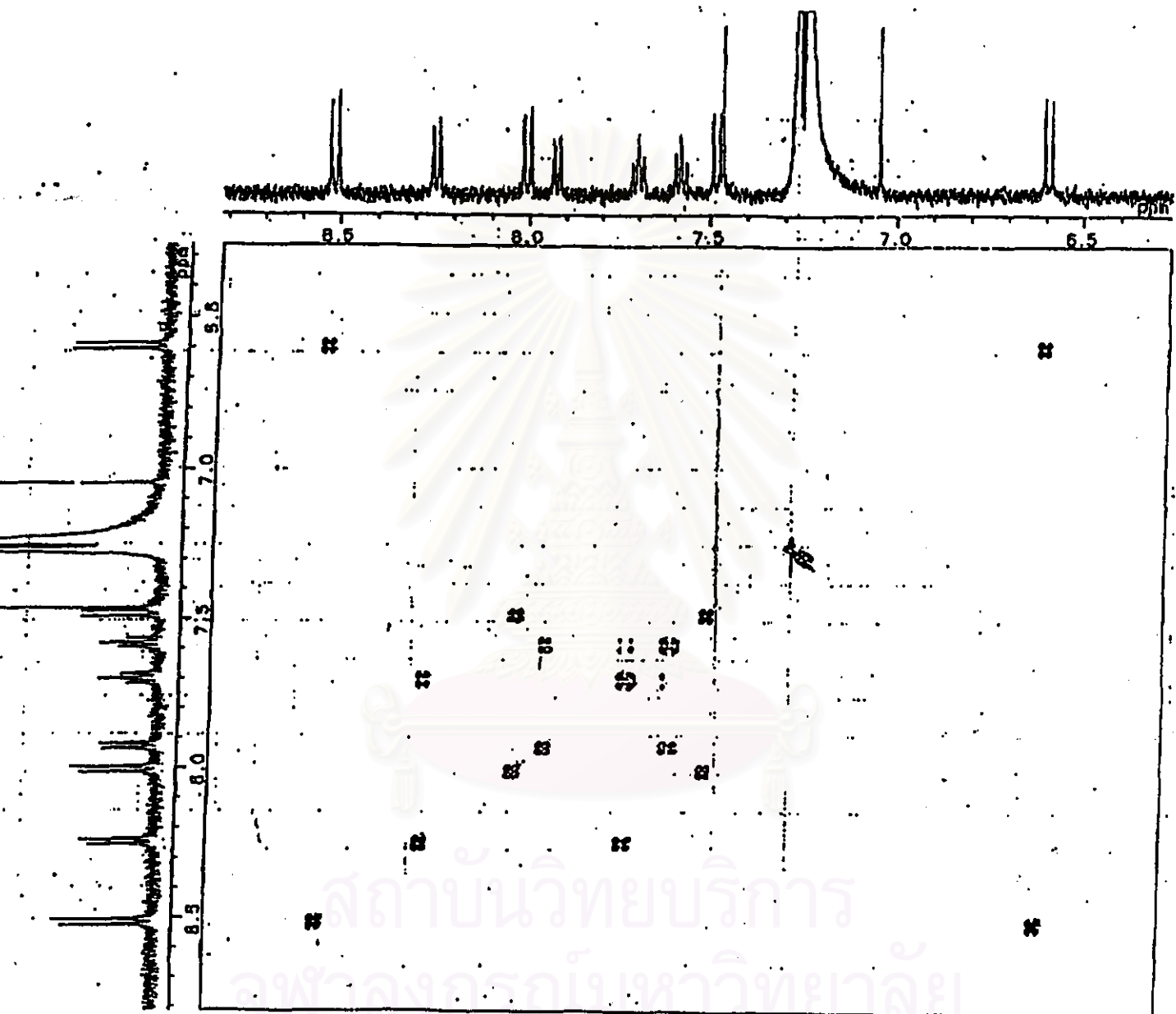


Figure 4.22 ^1H - ^1H COSY spectra of metabolite F1-IIIa formed from phenanthrene degradation by *Sphingomonas* sp. P2 grown in the presence of pyrene

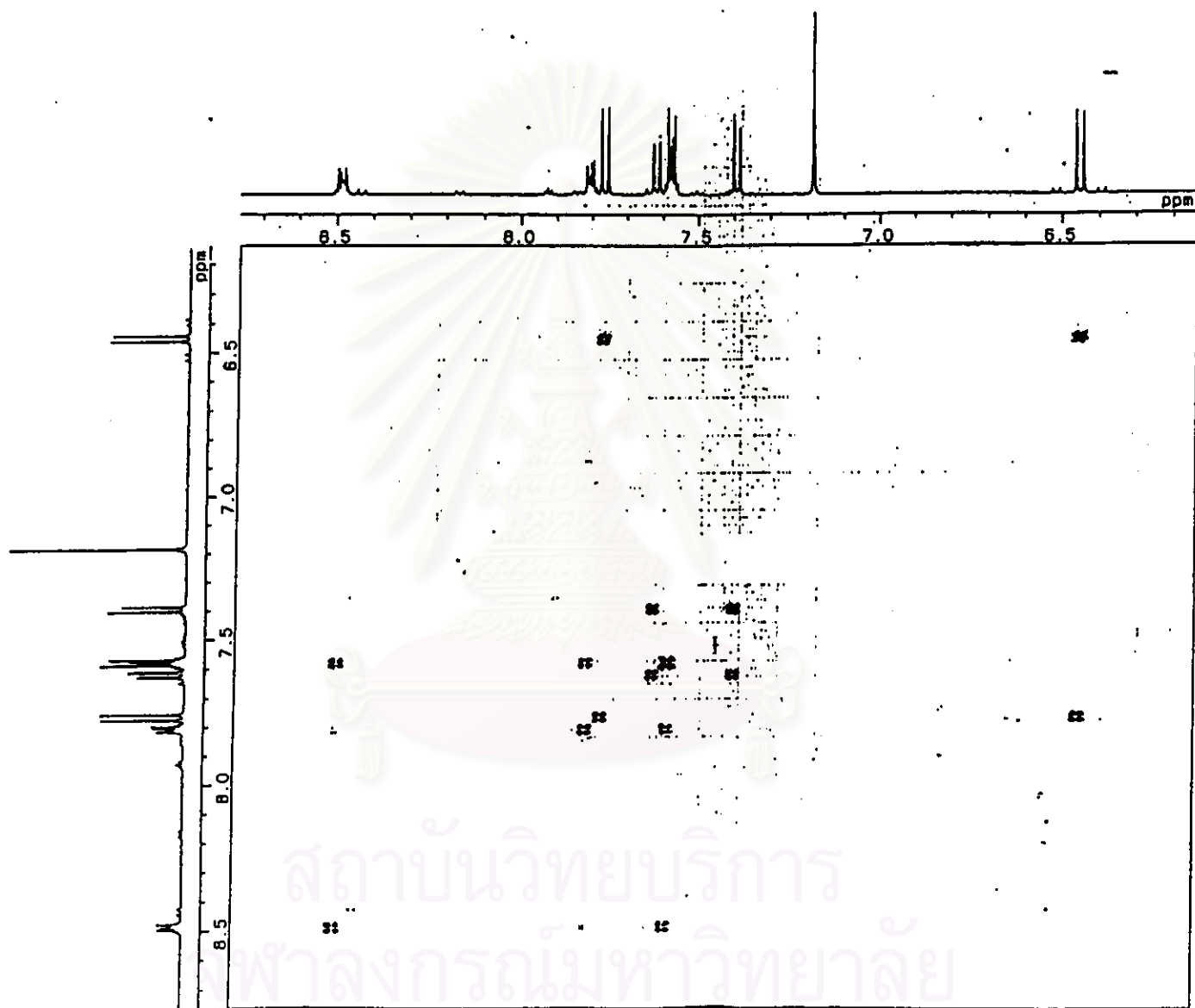


Figure 4.23 ^1H - ^1H COSY spectra of metabolite F1-IIIb formed from phenanthrene degradation by *Sphingomonas* sp. P2 grown in the presence of pyrene

To elucidate the structure of metabolite F1-IIIa, NOESY experiment was carried out. The spectral data (Figure 4.26) showed H-H long range connectivity that proton at 8.55 ppm coupled with proton at 8.22 ppm as well as proton at 7.88 ppm coupled with proton at 7.98 ppm (Figure 4.27)

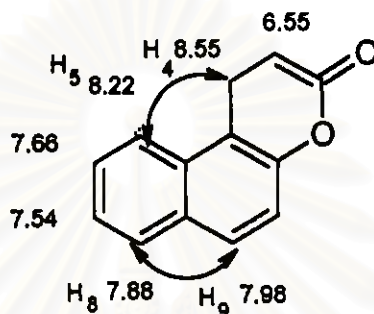


Figure 4.27 Most significant H-H long-range connectivity observed in NOESY of metabolite F1-IIIa

Combination of $^1\text{H-NMR}$, $^1\text{H-}^1\text{H COSY}$, NOESY and mass spectral data reveals structure of metabolite F1-IIIa as 5,6-benzocoumarin.

สถาบันวิทยบริการ
จุฬาลงกรณ์มหาวิทยาลัย

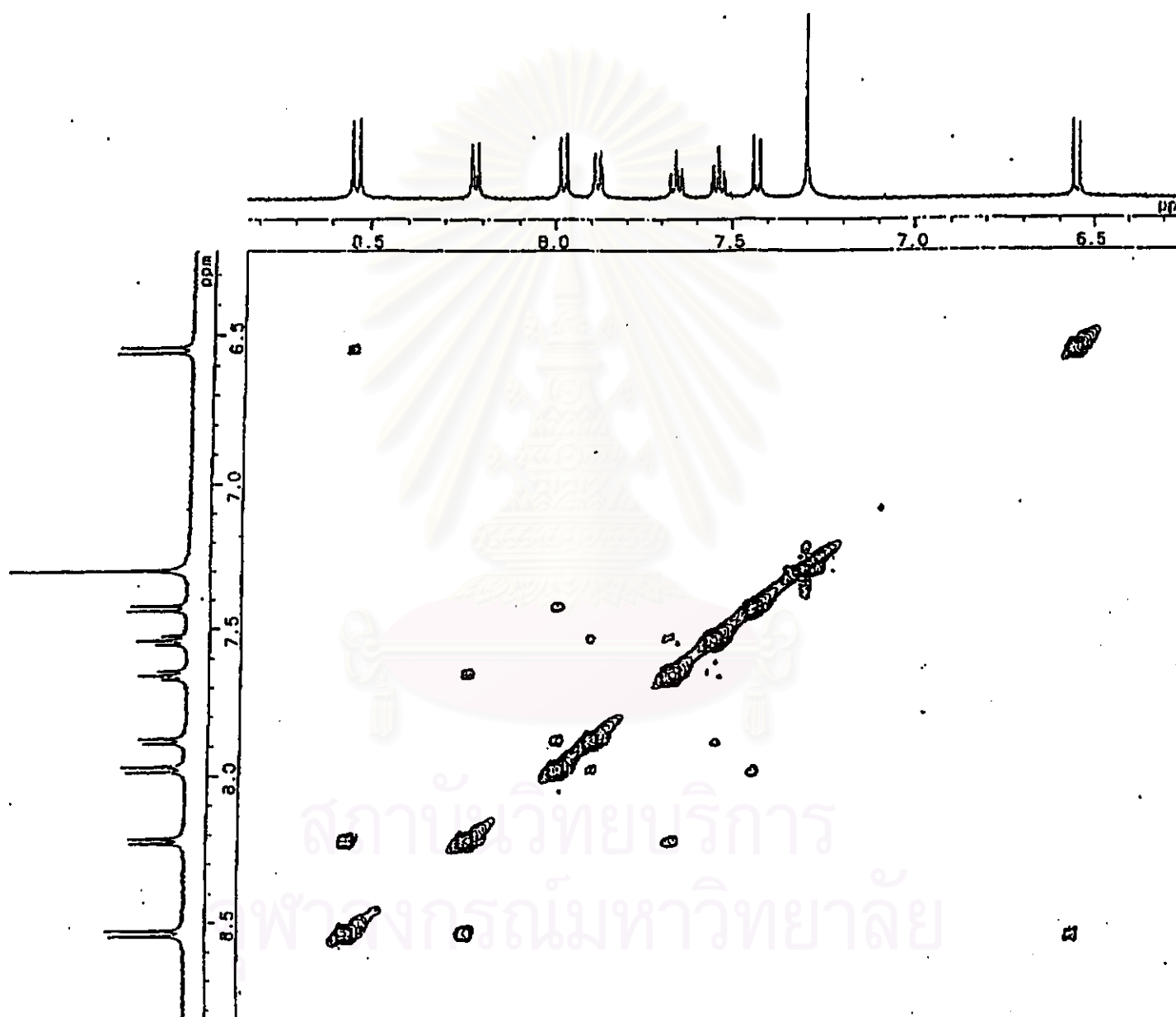


Figure 4.26 NOESY data of metabolite F1-IIIa formed from phenanthrene degradation by *Sphingomonas* sp. P2 grown in the presence of pyrene

To assign the structure of metabolite F1-IIIb, HMQC and HMBC experiments were conducted. HMQC spectra (Figure 4.28) showed H-C direct connectivity of this compound as depicted in Table 4.5 and HMBC spectra (Figure 4.29) showed long-range ^1H - ^{13}C correlations (Figure 4.30).

Table 4.5 The HMQC spectral data of metabolite F1-IIIb

Position	HMQC	
	δ_{H}	δ_{C}
1	7.83 (d)	144.2
2	6.49 (d)	116.0
5	8.50 (m)	122.4
8	7.84 (m)	127.8
6	7.61 (m)	127.2
7	7.61 (m)	128.8
9	7.66 (d)	124.5
10	7.44 (d)	123.6

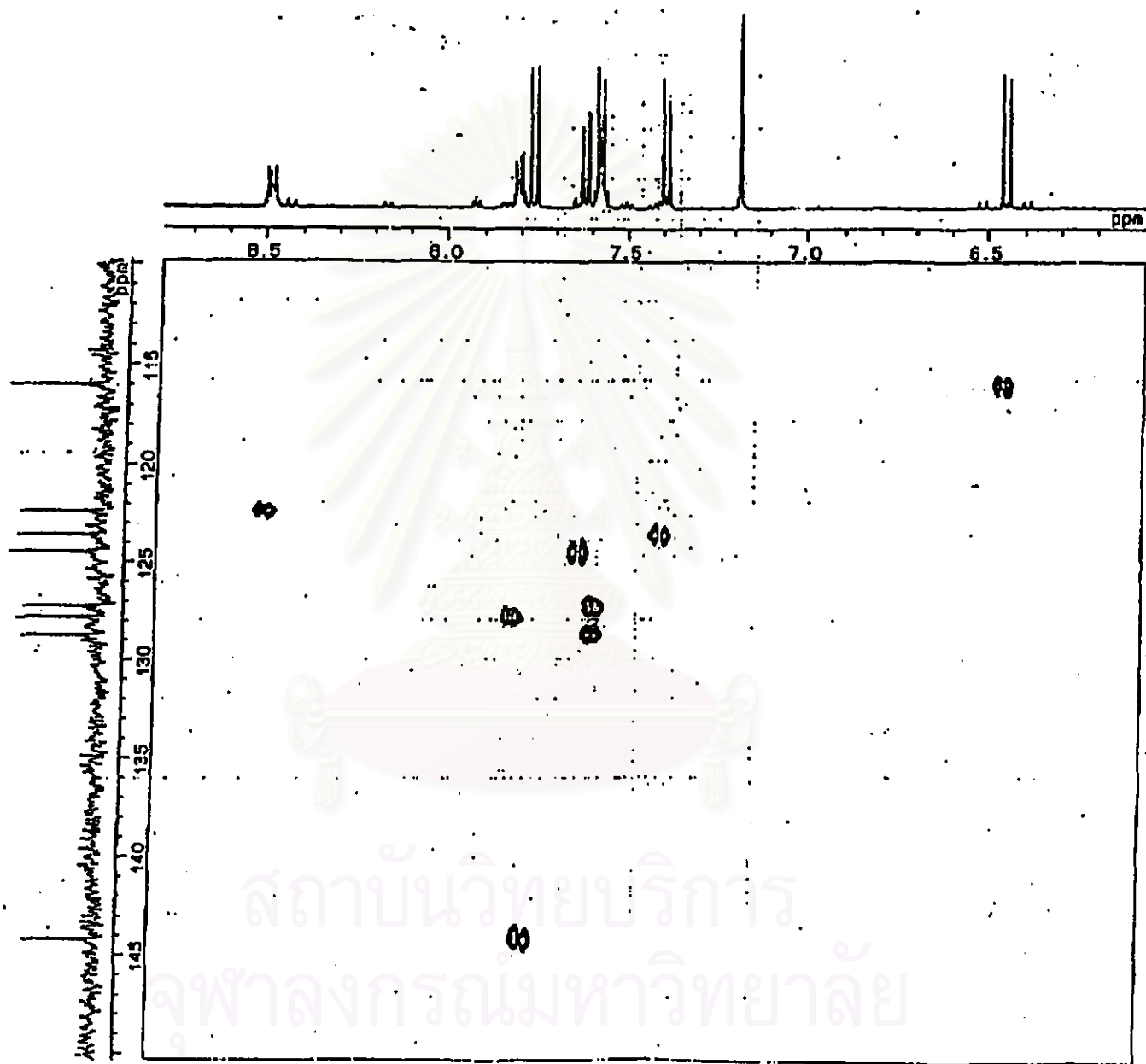


Figure 4.28 HMQC data of metabolite F1-IIIb formed from phenanthrene degradation by *Sphingomonas* sp. P2 grown in the presence of pyrene

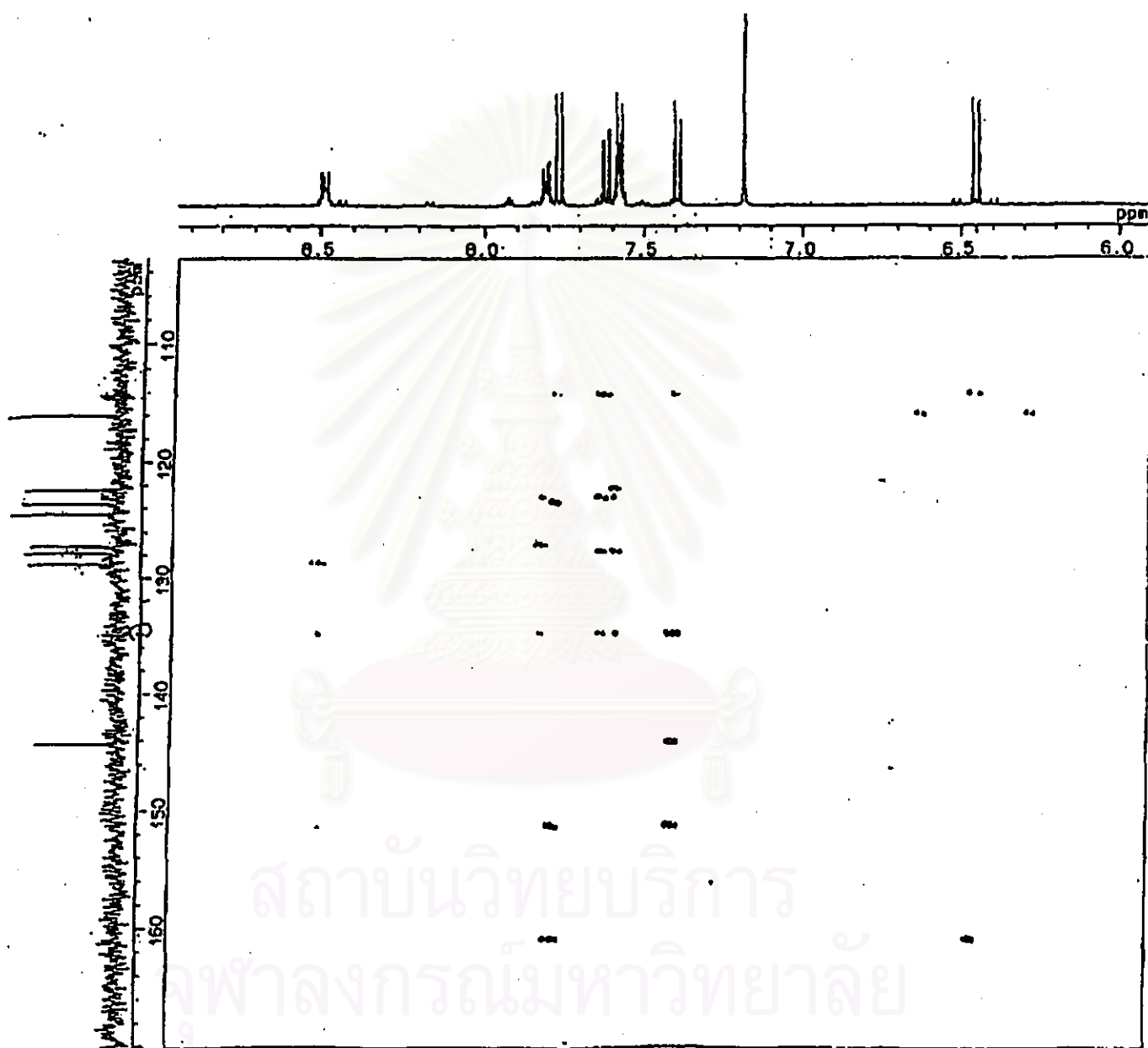


Figure 4.29 HMBC data of metabolite F1-IIIb formed from phenanthrene degradation by *Sphingomonas* sp. P2 grown in the presence of pyrene

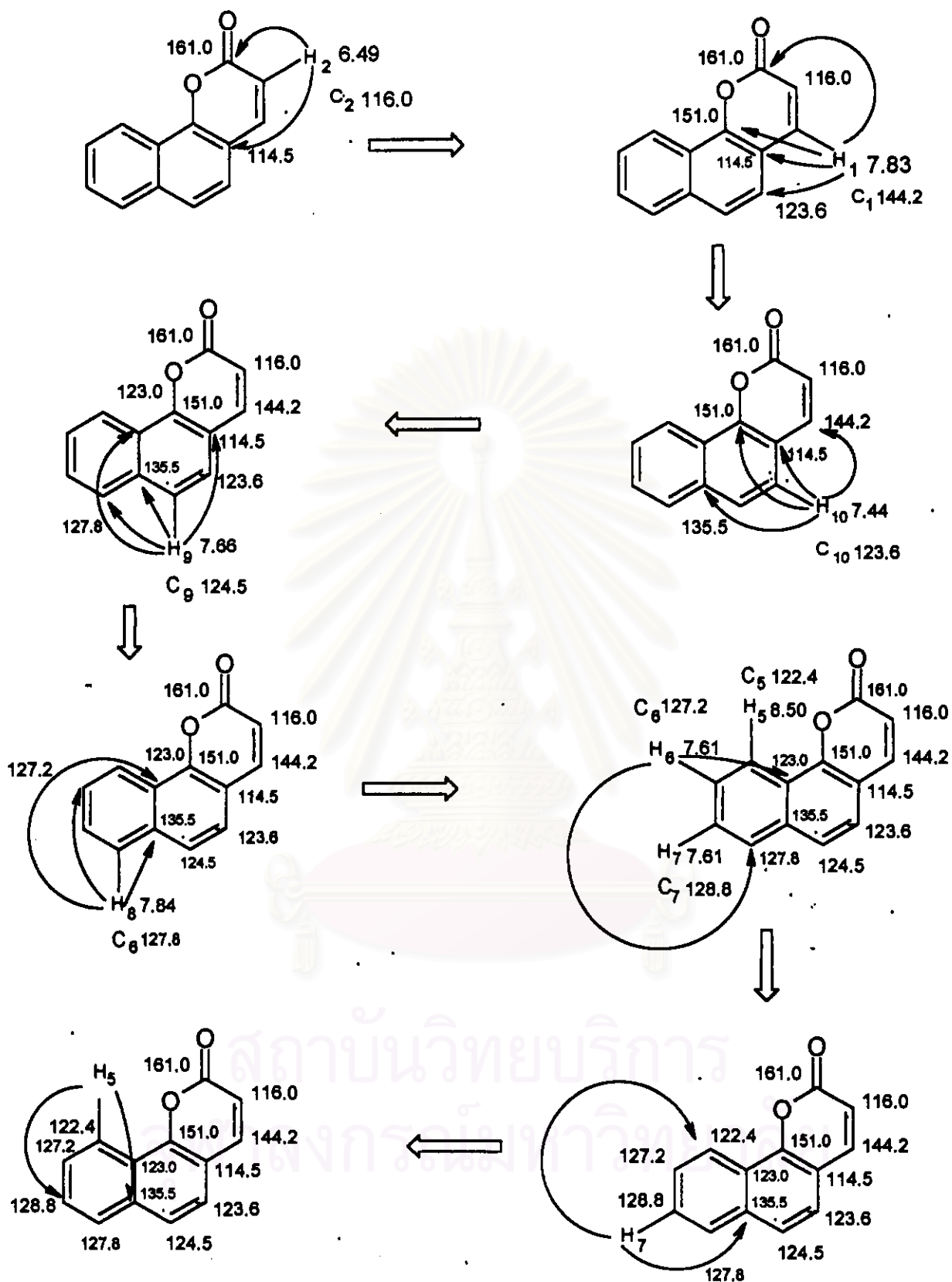


Figure 4.30 Most significant H-C long-range connectivity observed in HMBC of metabolite F1-IIIb

Metabolite F1-IVa

From ^1H NMR spectrum, metabolite F1-IVa showed similarity to authentic 1-hydroxy-2-naphthoic acid (Figures 4.31 and Table 4.6)

Table 4.6 ^1H NMR spectra data for metabolite F1-IVa and 1-hydroxy-2-naphthoic acid

Protons	δ_{H} (ppm)	
	Metabolite F1-IVa CDCl ₃ , 500 MHz	1-hydroxy-2-naphthoic acid CDCl ₃ , 89.56 MHz
H-3	7.69 (d)	7.80 (d)
H-4	7.20 (d)	7.42 (d)
H-5	7.80 (d)	7.93 (d)
H-6	7.42 (t)	7.62 (t)
H-7	7.48 (t)	7.67 (t)
H-8	8.30 (d)	8.33 (d)

สถาบันวิทยบริการ
จุฬาลงกรณ์มหาวิทยาลัย

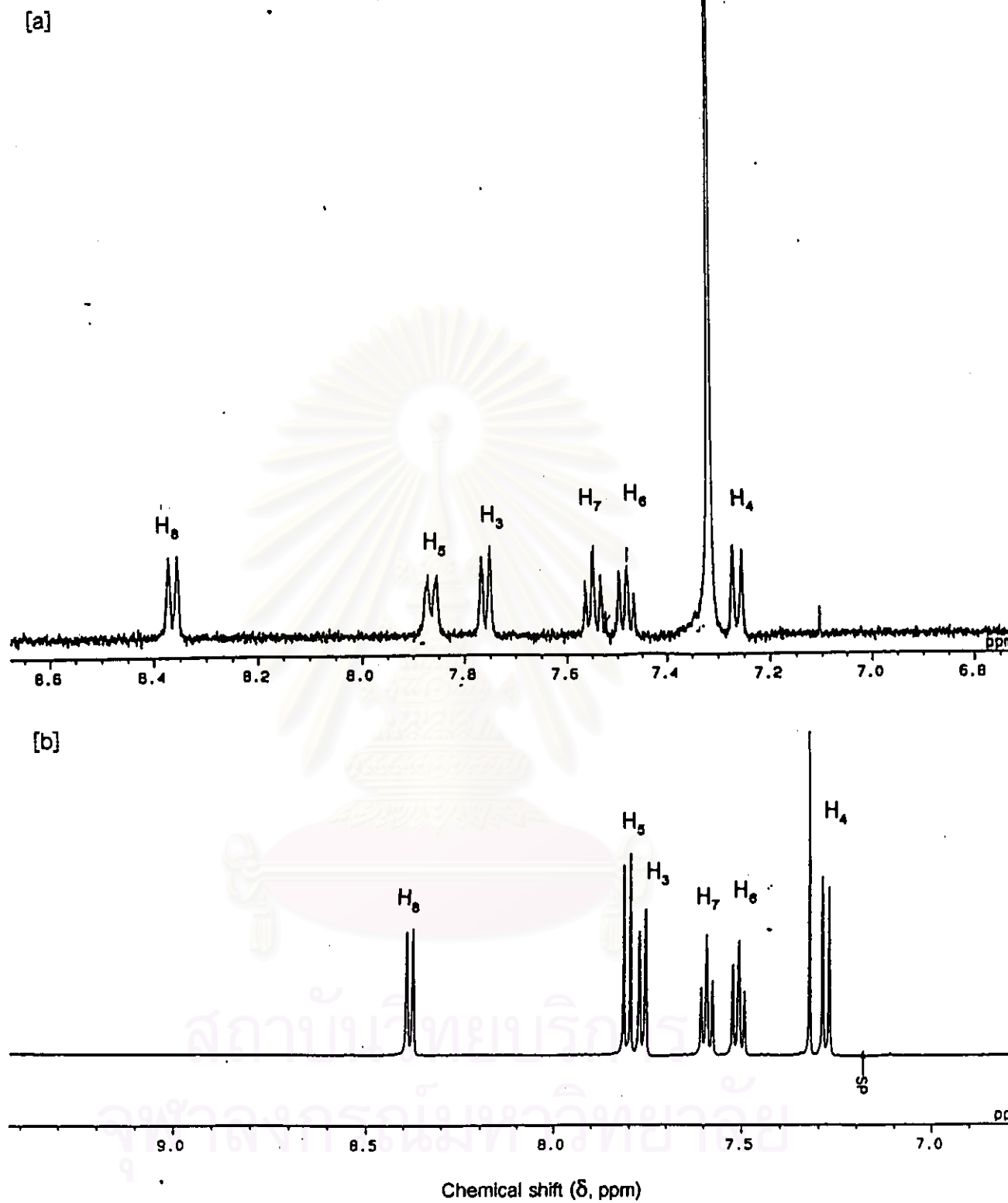


Figure 4.31 [a] $^1\text{H-NMR}$ spectrum of metabolite F1-IVa formed from phenanthrene degradation by *Sphingomonas* sp. P2 grown in the presence of pyrene and [b] standard [1-hydroxy-2-naphthoic acid] $^1\text{H-NMR}$ spectrum

The structure of metabolite F1-IVa was determined to be 1-hydroxy-2-naphthoic acid (Figure 4.31) based on the results of $^1\text{H-NMR}$.

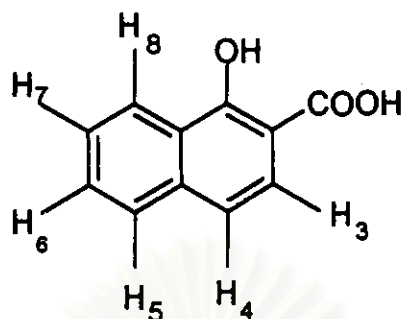


Figure 4.32 Structure of metabolite F1-IVa which is identical to that of 1-hydroxy-2-naphthoic acid

Unfortunately, the quantities and qualities of fractions F1-IIa and F1-IVb were not sufficient for further analyses.

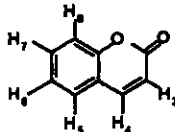
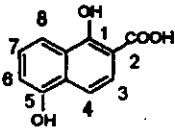
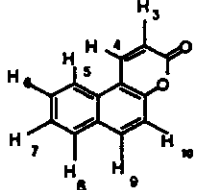
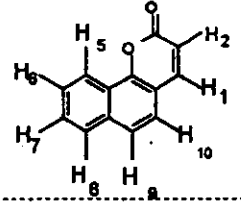
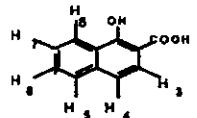
สถาบันวิทยบริการ
จุฬาลงกรณ์มหาวิทยาลัย

Table 4.7 GC-MS retention times, principal ions possible structures and elemental analysis of phenanthrene metabolites formed by *Sphingomonas* sp. P2 grown in the presence of pyrene

Metabolites	Retention time, <i>Rt</i> (min)	Principal ions and relative abundance (% base peak)	Identification or possible structure	elemental analysis
F1-I	6.2	146 (M ⁺ , 55), 118 (100), 90 (62), 63 (54)	Coumarin	C ₉ H ₆ O ₂
F1-IIb	10.5	218 (M ⁺ , 23), 186 (100), 168 (6), 158 (26), 130 (65), 102 (24), 77 (12)		C ₁₂ H ₁₀ O ₄ ^a
	10.2	232 (M ⁺ , 32), 200 (100), 185 (47), 172 (15), 157 (86), 144 (16), 129 (36), 115 (14), 101 (52), 75 (23)		C ₁₃ H ₁₂ O ₄ ^a
F1-IIIa	10.4	196 (M ⁺ , 49), 168 (100), 139 (80), 113 (12), 70 (12), 63 (15)	Benzocoumarin	C ₁₃ H ₈ O ₂
F1-IIIb	10.2	196 (M ⁺ , 49), 168 (100), 139 (70), 113 (15), 63 (18)	Benzocoumarin	C ₁₃ H ₈ O ₂

^a GC-MS data for methyl derivatives

Table 4.8 Proton and carbon chemical shifts of phenanthrene metabolites formed by *Spingomonas* sp. P2 grown in the presence of pyrene

Metabolite	Chemical Shifts (δ) ^a		Identification
	¹ H NMR	¹³ C NMR	
I	7.77 (H-4, d, $J=9.5$ Hz), 7.56 (H-7, t, $J=8.0$ Hz), 7.52 (H-5, d, $J=8.0$ Hz), 7.36 (H-8, d, $J=8.0$ Hz), 7.30 (H-6), 6.45 (H-3, d $J=9.5$ Hz)	ND	Coumarin 
F1-IIb	7.53-7.58 (3H, m), 7.11 (2H, dd)	174.2 (COOH), 159.1 (C-1), 154.6 (C-5), 131.6 (C), 129.0 (C-7), 125.8(C), 122.2 (C-3), 120.7 (C-4), 117.9 (C-8), 107.2 (C-2), 105.2 (C-6)	1,5-dihydroxy-2-naphthoic acid 
F1-IIIa	8.54 (H-4, d, $J=9.7$ Hz), 8.22 (H-5, d, $J=8.0$ Hz), 7.98 (H-9, d, $J=9.0$ Hz), 7.88 (H-8, d, $J=8.0$ Hz), 7.66 (H-6, t, $J=8.0$ Hz), 7.54 (H-7, t, $J=8.0$ Hz), 7.43 (H-10, d, $J=9.0$ Hz), 6.55 (H-3, d, $J=9.7$ Hz)	ND	5,6-benzocoumarin 
F1-IIIb	8.50 (H-5, m), 7.84 (H-8, m), 7.83 (H-1, d, $J=9.5$ Hz), 7.66 (H-9, d, $J=8.5$ Hz), 7.61 (H-6, 7, m), 7.44 (H-10, d, $J=8.5$ Hz), 6.49 (H-2, d, $J=9.5$ Hz)	161.0 (C-3), 151.0 (C), 144.2 (C-1), 135.5 (C), 128.8 (C-7), 127.8 (C-8), 127.2 (C-6), 124.5 (C-9), 123.6 (C-10), 123.0 (C), 122.4 (C-5), 116.0 (C-2), 114.5 (C)	7,8-benzocoumarin 
F1-IVa	8.30 (H-8, d), 7.80 (H-5, d), 7.69 (H-3, d), 7.48 (H-7, t), 7.42 (H-6, t), 7.20 (H-4, d)	ND	1-hydroxy-2-naphthoic acid 

^a Determined at 500 MHz (¹H NMR) or 125 MHz (¹³C NMR) in 10% CD₃OD in CDCl₃. Chemical shift multiplicities are abbreviated as follows: d, doublet; t, triplet; m, multiplet; dd, doublet of doublet; (C), ¹³C chemical shifts of quaternary carbons; ND, not determined.

4.2 Identification of metabolites from degradation of fluoranthene via co-metabolism with phenanthrene by *Sphingomonas* sp. P2

4.2.1 Partial purification by silica gel open column chromatography

After cultivation of *Sphingomonas* sp. P2 in CFMM/phe/flu for 4 days, bacterial cells separation and extraction of 5 liter supernatant with ethyl acetate according to the procedure shown in Figure 3.2 were performed. The acidic extract obtained (1.03 g) was partially purified by silica gel open column chromatography, 12 fractions were collected (Table 4.9), dehydrated over anhydrous Na_2SO_4 , evaporated to 10 ml and characterized via TLC to identify fractions containing metabolites. Results are shown in Figure 4.33.

Table 4.9 Dry weight of each fraction obtained from silica gel open column chromatography of the acidic extract

Fraction	Eluent (%by volume)		Dry weight (mg)
	<i>n</i> -Hexane	Ethyl acetate	
1	100	0	0.03
2	90	10	9.30
3	80	20	18.30
4	70	30	22.46
5	60	40	107.67
6	50	50	77.25
7	40	60	272.83
8	30	70	114.75
9	20	80	54.63
10	10	90	33.09
11	0	100	17.17
12	100% Methanol		44.02

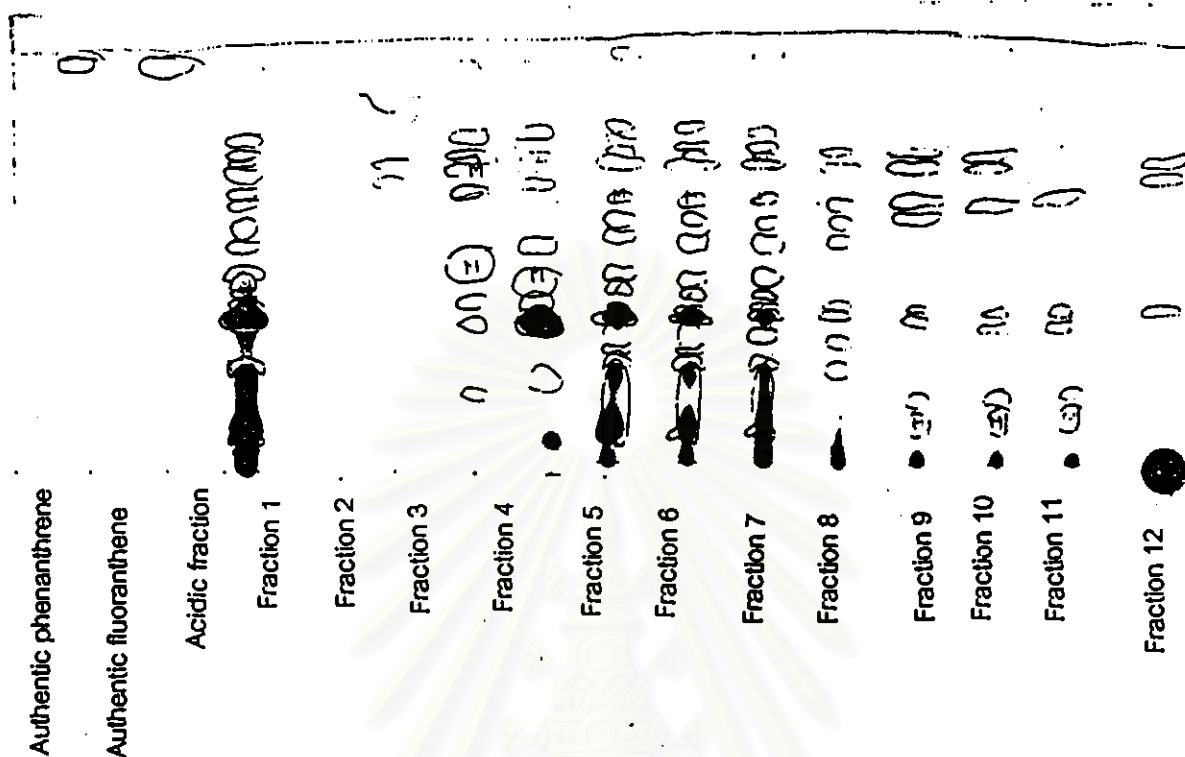


Figure 4.33 TLC chromatogram of each fraction after partial purification by silica gel open column chromatography. TLC-developing solvent system was toluene, dioxane and acetic acid (90:25:4,v/v/v) solvent system.

TLC analyses revealed that metabolites were found in all fractions. However, fractions 3 to 7 designated A1 to A5 were chosen to further separation of metabolites.

4.2.2 Purification of the metabolites by HPLC and TLC

The fractions collected were evaporated to dryness and redissolved in methanol to the concentration of 1 mg/10 μ l. These fractions were subjected to reversed phase HPLC eluted with linear gradient solvent system. The HPLC elution profiles are shown in Figure 4.34.

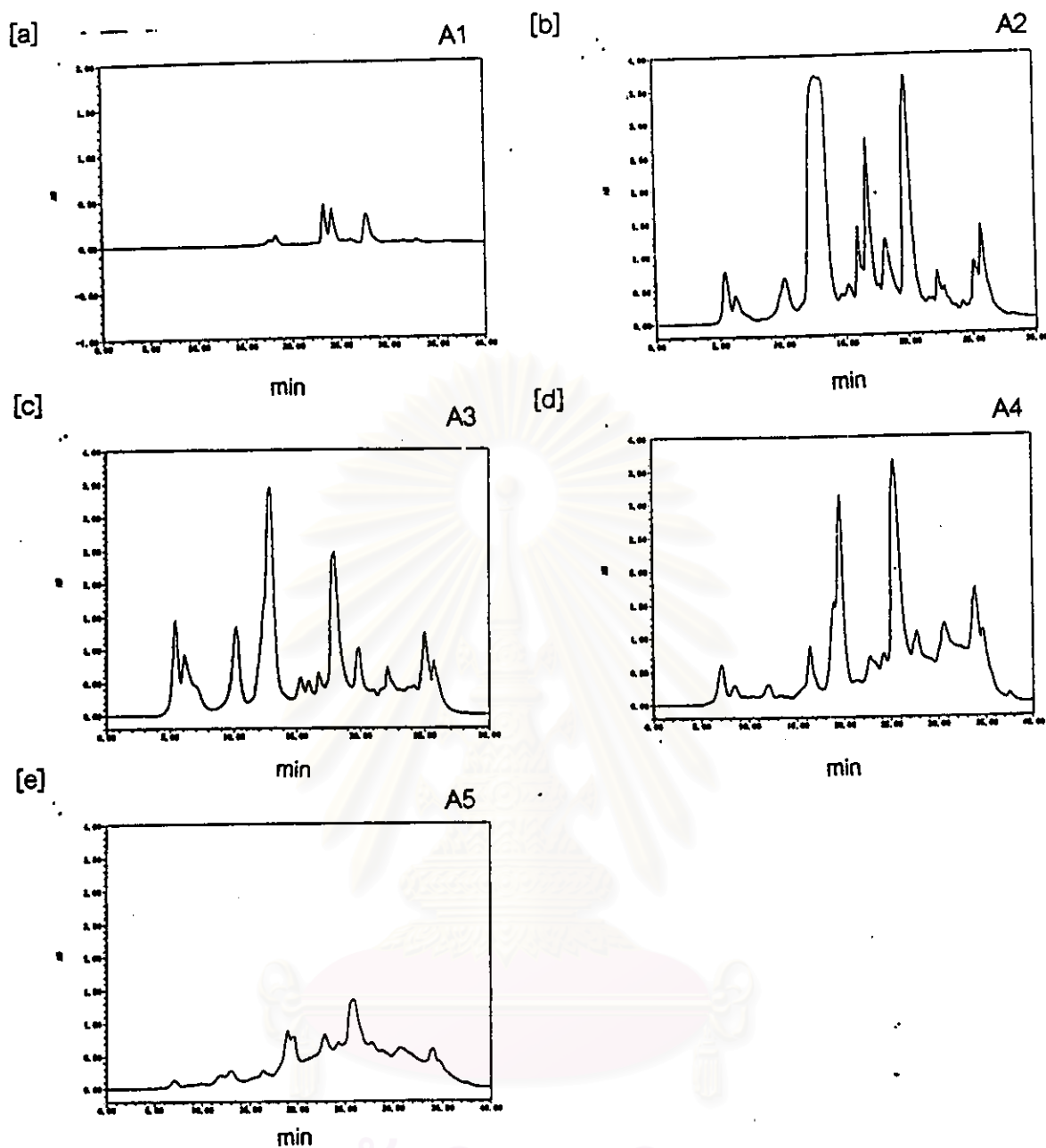


Figure 4.34 HPLC chromatogram of fractions A1 to A5 separated on an ODS-4253-D column using a methanol- water linear gradient solvent system (50 to 100 % [v/v] methanol containing 1% acetic acid) for the elution

When comparing the HPLC chromatogram of fraction A2 with that of fraction F1 (Figure 4.35), certain distinct metabolites could be found suggesting fractions A2-I, A2-II and A2-III.

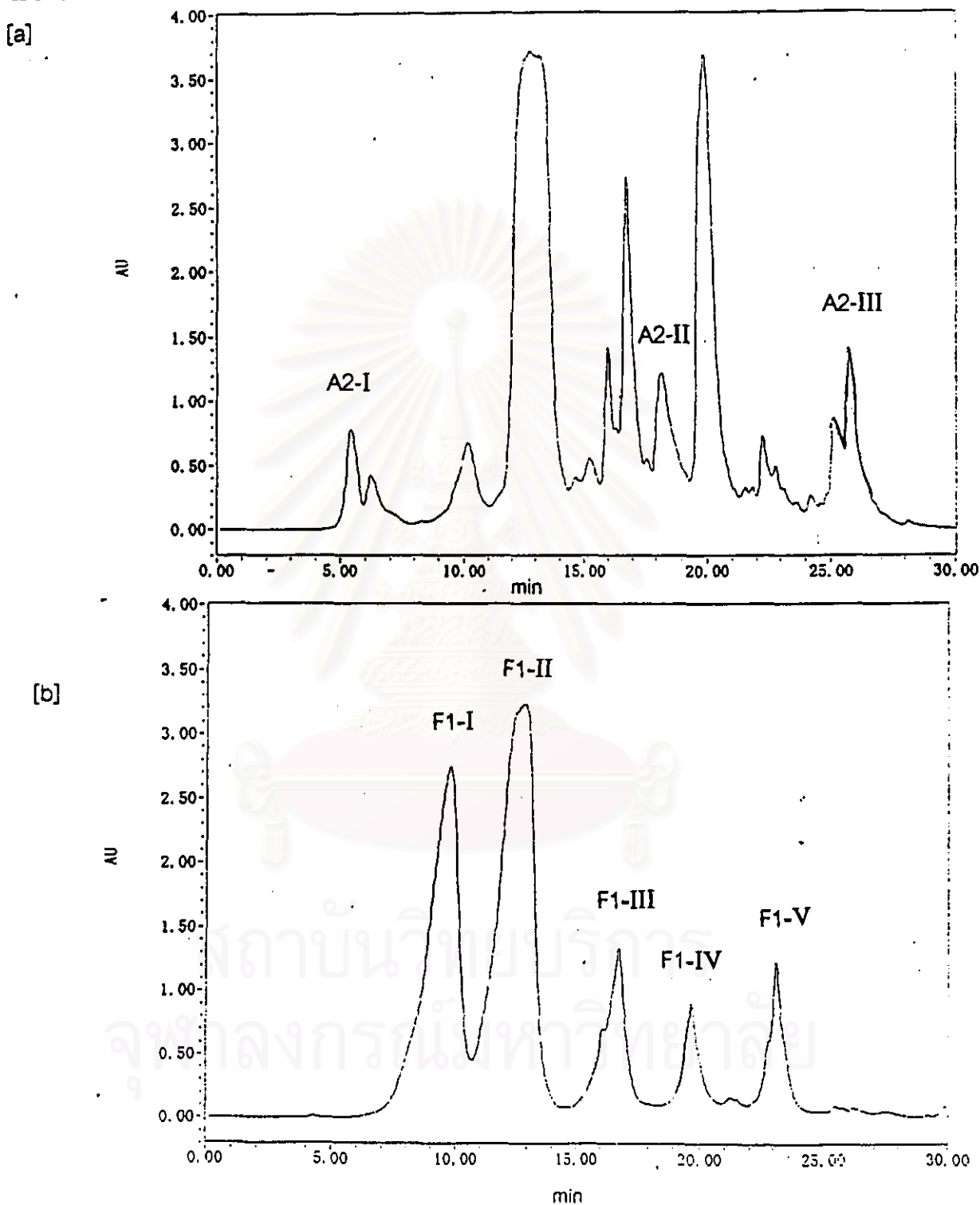


Figure 4.35 Comparison of HPLC elution profile of [a] phenanthrene+fluoranthene and [b] phenanthrene+pyrene experiments

However, after purification of metabolite A2-I via reversed phase HPLC with isocratic solvent system and purification of metabolites A2-II and A2-III via reversed phase HPLC with isocratic solvent system and preparative TLC, both quantities and qualities of these compounds were not sufficient for further analyses.

4.3 Genes involved in phenanthrene metabolism

To study dioxygenase genes, polymerase chain reaction (PCR) and shot gun cloning experiment were carried out.

4.3.1 Detection of consensus sequence of iron-sulfur protein large subunit (ISP α) of dioxygenase in *Sphingomonas* sp. P2

In order to detect consensus sequence of ISP large subunit of dioxygenase in *Sphingomonas* sp. P2, PCR experiment using pairs of several primers; nahAc, phnAc, modified pPAH, and Rieske type primers were conducted.

nahAcforward and nahAcreverse primers having sequences corresponding to nucleotide number 63-82 and 1036-1055 of nahAc gene, respectively (Lloyd-Jones *et al.*, 1999) (encodes ISP large subunit of dioxygenase in *Pseudomonas putida* G7) (Simon *et al.*, 1993) were used as the first pair of oligonucleotide primers. These primers are specific for the conserved nahAc sequences of nah-like genotypes, including nahAc gene from *P. putida* G7, nahAc gene from *P. putida* NCIB9816-4 (Simon *et al.*, 1993), ndoB gene from *P. putida* NCIB9816 (Yang *et al.*, 1994), doxB gene from *Pseudomonas* sp. C18 (Denome *et al.*, 1993) and pahAc gene from *P. putida* OUS82 (Kiyohara *et al.*, 1994). The amino acid sequence homology of the gene products in this group is approximate 80% (Laurie and Lloyd-Jones *et al.*, 1999). PCR was carried out by using total DNA of *Sphingomonas* sp. P2 and plasmid pDI1, a plasmid carrying pahAc gene from *P. putida* (Kiyohara *et al.*, 1994), as DNA templates. Expected size of PCR products was 992 bp. The results revealed that the positive control showed the expected size of DNA fragment whereas no PCR product was obtained with total DNA of *Sphingomonas* sp. P2 as a template.

Thus the second pair of generate primers which correspond to gene encoding ISP large subunit of dioxygenase and differ from primers from *nahAc*-like group was used for PCR experiment. These were *phnAC*forward and *phnAcreverse* primers, sequences correspond to nucleotide number 82-100 and 1057-1076 of *phnAc* gene from *Burkholderia* sp. RP007 (Lloyd-Jones *et al.*, 1999). The homology of *PhnAc* and *NahAc*-like ISP large subunit is about 56 % (Laurie and Lloyd-Jones *et al.*, 1999). PCR using total DNA of *Sphingomonas* sp. P2. and *Burkholderia* sp. RP007 as DNA templates were carried out to amplify 994 bp DNA fragments. However, there was still no PCR product generated from this pair of primer.



สถาบันวิทยบริการ
จุฬาลงกรณ์มหาวิทยาลัย

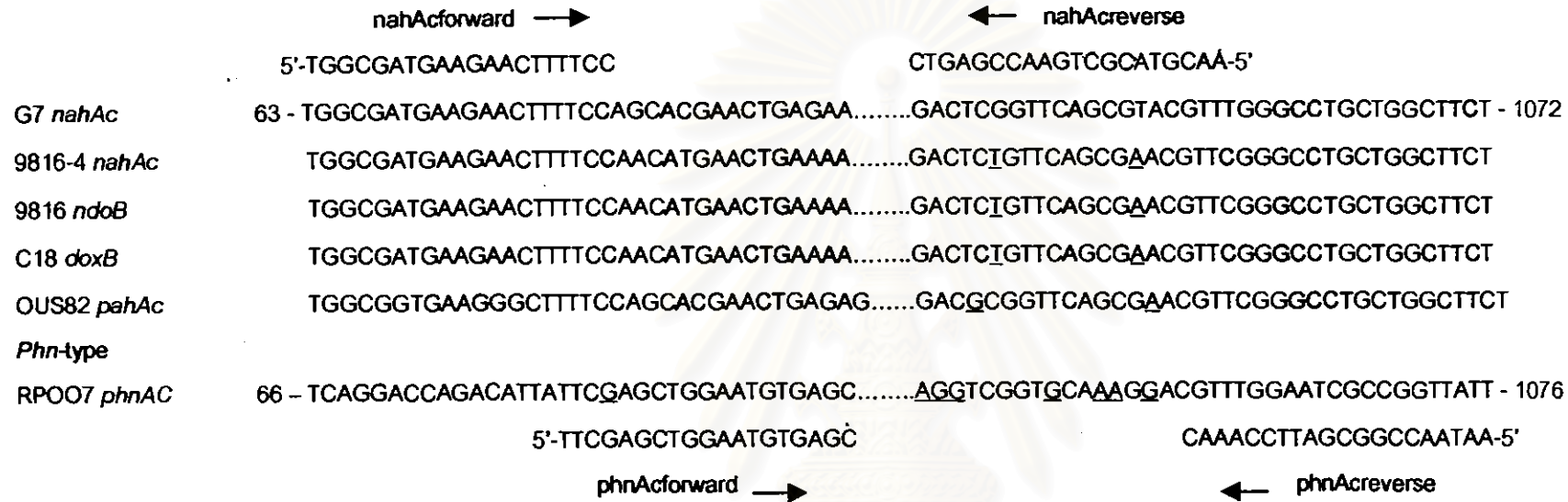
nah-like group

Figure 4.36 Alignment of partial nucleotide sequences encoding for the α -subunits of the initial PAH dioxygenase enzyme from naphthalene- and phenanthrene-degrading bacteria. Sequences gaps are shown as dots. The nahAcforward/nahAcreverse primers from *P. putida* G7 are shown above the alignment and phnAcforward/phnAcreverse primers from *Burkholderia* sp. RPO07 are shown below the alignment (Lloyd-Jones *et al.*, 1999).

Furthermore, the third pair of primers which are degenerate primers were used to detect gene encoding ISP large subunit of dioxygenase. These degenerate primers were pPAHforward and pPAHreverse primers modified from those described by Hedlund *et al.* (1999). They were described from amino acid positions 93-107 and 316-327 of naphthalene dioxygenase ISP large subunit from *P. putida* G7 (Simon *et al.*, 1993). These degenerate primers were used with the intention to amplify 630 bp DNA fragments (approximately one-half of the 1,245 bp-*nahAc* gene (Simon *et al.*, 1993). From this PCR experiment, we could not obtain PCR product yet.

In addition, another degenerate primers were also used. The degenerate primer pools were derived from the highly conserved amino acid sequence of the ISP α [2Fe-2S]-Rieske center of *P. putida* G7 (Simon *et al.*, 1993), *Pseudomonas* sp. C18 (Denome *et al.*, 1993), *P. putida* OUS82 (Kiyohara *et al.*, 1994), *P. putida* F1 (Zylstra and Gibson, 1989), *Pseudomonas* sp. LB 400 (Erlison and Mondello, 1992), *Pseudomonas* sp. KKS102 (Kikuchi *et al.* 1994) and *P. fluorescens* IP01 (Aoki *et al.*, 1996). These primers namely Rieskeforward and Rieskereverse primers were derived from amino acid sequences CRHRGM (position 80-85) and CSYHGW (position 100-105), respectively. Using these degenerate primers and the DNA template from *Sphingomonas* sp. P2, the PCR product of 78 bp was expected to be obtained. Nevertheless, no expected size of PCR product could be obtained.

Using PCR technique with several primers mention above, gene encoding ISP large subunit of dioxygenase from *Sphingomonas* sp. P2 could not be obtained. Consequently, shot gun cloning experiment was carried out as an alternative method to obtain gene involving in phenanthrene degradation in this bacterium.

4.3.2 Shot gun cloning experiment

Shot gun cloning is a useful method to obtain particular gene from simple organism. A very large number of DNA inserts was incorporated into cloning vectors. Such a collection of insert molecules which represents the entire genome of an organism (gene library) was screened for particular gene by using specific features of this gene.

In order to obtain gene involved in phenanthrene degradation of *Sphingomonas* sp. P2., shot gun cloning was carried out. Total DNA of *Sphingomonas* sp. P2. and plasmid pUC18, pUC19, pUC118 and pUC119 were completely digested with one of restriction enzymes; *Bam*HI, *Eco*RI, *Hind*III, *Pst*I, *Sph*I or *Sal*I. According to previous study, genes encoding the lower and upper of PAH degradation pathways are arranged in two respective polycistronic operons (Sutherland, 1995). Each operon possesses nucleotide about 10 kb (Laurie and Lloyd-Jones, 1999a and b). Thus 1-10 kb DNA fragments were chosen to ligate with appropriate digested plasmids. After ligation and transformation of recombinant plasmids into *E. coli* JM109, about 3,000 white clones were obtained on LB-Ap-IPTG/X-Gal plates.

These white clones were replicated on LB-Ap plates and further screened for aromatic oxygenase and extradiol dioxygenase activities. In order to detect the activity all white clones were screened for the formation of indigo colour (Ensley *et al.*, 1983). For this purpose, LB or 2xYT-Ap-IPTG liquid medium were used to cultivate the white clones. These media contain tryptophan which converted to indole by tryptophanase in *E. coli*, indole will be served as a substrate for dioxygenase. Indigo colour will be formed after transformation of indole to indigo by dioxygenase (Ensley *et al.*, 1983). If *E. coli* contains recombinant plasmid carrying aromatic oxygenase gene, indole will be converted to indigo. After incubation for 16-18 hr, the colour of media will change to green when blue colour of indigo was mixed with yellow colour of medium. However, no positive clone was found from 3,000 white clones, while the positive control; *E. coli* JM109 containing pDI1 plasmid showed colour of indigo (Figure 4.37).

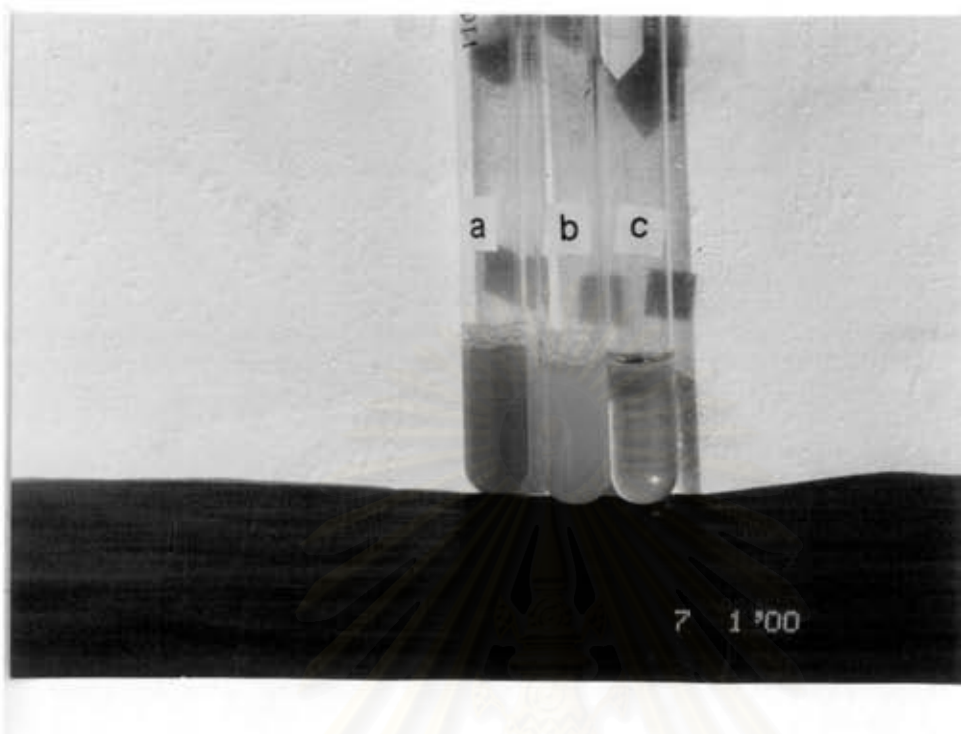


Figure 4.37 [a] Blue colour of indigo formed by *E. coli* JM109 carrying pDI1 plasmid [b] *E. coli* JM109 [c] Colour of LB- α -IPTG medium



Furthermore, *meta*-cleavage dioxygenase activity was also used for screening. Each colony of all white clones on LB-Ap-IPTG plates was screened by being dropped with 20 μ l of 50 mM 2,3-dihydroxybiphenyl dissolved in DMSO. After 15 min, yellow colour of *meta*-cleavage product will appear if clone possesses this activity (Kimura *et al.*, 1996). The results revealed that only *Sphingomonas* sp. P2 (positive control) showed yellow colour of *meta*-cleavage product (Figure 4.38) whilst no single positive clone was found from 3,000 tested clones.

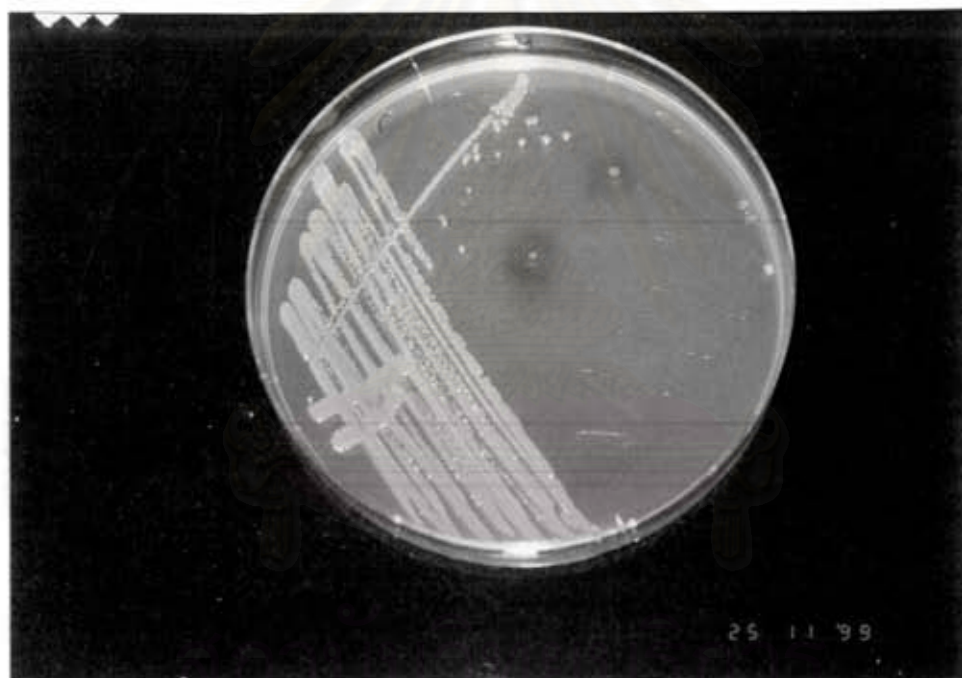


Figure 4.38 Yellow colour of *Sphingomonas* sp. P2 formed after being dropped with 50 mM of 2,3-dihydroxybiphenyl dissolved in DMSO